

DESIGN OF AN EFFICIENT CONDENSER FOR TUMBLE DRYERS

by

Onur Hartoka

Submitted to the Institute of Graduate Studies in  
Science and Engineering in partial fulfillment of  
the requirements for the degree of  
Master of Science  
in  
Mechanical Engineering

Yeditepe University

2009

DESIGN OF AN EFFICIENT CONDENSER FOR TUMBLE DRYERS

APPROVED BY

Assoc.Prof.Dr. Hojin Ahn  
(Thesis Supervisor)

.....

Prof. Dr. Oktay Özcan

.....

Asst. Prof. Esra Sorgüven

.....

DATE OF APPROVAL: 29/12/2009

## ACKNOWLEDGEMENTS

Foremost, I would like to thank my advisor Assoc. Prof. Dr. Hojin Ahn for providing me with the opportunity to complete my master of science thesis at Yeditepe University in a SANTEZ reserch project in collaboration with Arçelik A.Ş. He has been actively interested in my work and has always been available to advise me. I am very grateful for his patience, motivation and also great knowledge on the subject that, taken together, made him a great mentor.

I would also like to include my gratitude to Gökhan Özgürel, R&D Manager, and also to Ph.D. Deniz Şeker, R&D Team Leader who have enabled this research work within Arçelik A.Ş. and provided support for this research at the R&D Department along the way.

I would specially like to thank my colleague Yavuz Şahin for his extremely valuable partnership in discussion throughout the project. He has been my greatest supporter.

I would also like to thank Mehmet Kaya and Murat Elgün for their great support on the condenser testing unit. Their skills in handling sophisticated equipments made it very easy for me to handle with technical problems.

Furthermore I am deeply indebted to all other colleagues at Cleaning Technologies Department of Arçelik R&D who have provided a warm environment for me and shared their experience on problems encountered throughout the project.

Finally, I would like to thank my parents Cahit and Gülsemin Hartoka and my brother Hakan Hartoka for their never-ending support.

## **ABSTRACT**

### **DESIGN OF AN EFFICIENT CONDENSER FOR TUMBLE DRYERS**

Air condenser tumble dryers are those of the most energy consuming home appliances. Therefore, improving the performance of the condenser tumble dryers has recently drawn much attention in today's world where the energy reserves continuously reduce. Among the various components of the tumble dryers, the condenser is the most important one. The first object of this study was to determine the factors that affect the performance of the condenser which is of the air-to-air heat exchangers. For this purpose a simple air condenser dryer energy model was developed and the effect of the condenser on energy consumption was investigated. A condenser testing unit was designed and constructed to measure the performance of the condensers. The test matrix was formed according to a "Design of Experiment (DOE)." The tests of the existing benchmark condenser were conducted to determine the factors that affect the condenser performance. In the second part of the study two new condensers were designed and prototyped. One of two new condensers was tested in the condenser testing unit and the results were compared with the existing benchmark condenser. Finally, three condensers, that is, the existing benchmark condenser and two newly designed condensers, were tested in a benchmark air condenser tumble dryer. The test results showed that one of the newly designed condensers had much better performance than the benchmark condenser in terms of the condenser efficiency, the condensation rate, the water collecting efficiency and the energy consumption values, while the other newly designed condenser was slightly better than the benchmark one.

## ÖZET

### ÇAMAŞIR KURUTMA MAKİNALARI İÇİN VERİMLİ KONDENSER TASARIMI

Doğal enerji kaynaklarının giderek azaldığı günümüz dünyasında en fazla enerji tüketen beyaz eşyalardan biri olması nedeni ile yoğunlaştırıculu çamaşır kurutma makinalarının performanslarını iyileştirmek için yapılan çalışmalar büyük önem taşımaktadır. Bu çalışmanın ilk amacını çamaşır kurutma makinalarının en önemli komponenti olan yoğunlaştırıcunun (kondenserin) performansını etkileyen faktörlerin belirlenmesi oluşturmuştur. Bu amaçla ilk olarak basit bir sayısal kurutucu modeli oluşturularak kondenserin kurutucu enerji tüketimi üzerine olan etkisi incelenmiştir. Mevcut ve geliştirilecek olan kondenserlerin test edilebilmesi amacıyla bir kondenser test düzeneği tasarlanıp kurulmuştur. Bir deney tasarımı oluşturularak mevcut kondenserin performansını etkileyen faktörler belirlenmiştir. Çalışmanın ikinci adımında iki farklı kondenser tasarlanıp prototipleri ürettirilmiştir. Prototip kondenserlerden biri kondenser test ünitesine bağlanarak performans sonuçları mevcut kondenser ile karşılaştırılmıştır. Çalışmanın son adımında ise biri mevcut, diğerleri tasarlananlar olmak üzere üç kondenser de çamaşır kurutma makinasına takılarak test edilmiştir. Sonuçta tasarlanan kondenserlerden ilkinin kondenser verimi, yoğunlaşma hızı, su toplama verimi ve enerji tüketimi değerleri bakımından mevcut kondensere çok daha iyi sonuçlar verdiği tespit edilmiştir. Tasarlanan ikinci kondenserin performansının ise ilk kondenser kadar olmasada mevcut kondensere daha iyi olduğu görülmüştür.

## TABLE OF CONTENTS

ACKNOWLEDGEMENTS.....	iii
ABSTRACT.....	iv
ÖZET .....	v
TABLE OF CONTENTS.....	vi
LIST OF FIGURES .....	viii
LIST OF TABLES.....	xii
LIST OF SYMBOLS .....	xiv
1. INTRODUCTION .....	1
1.1. BACKGROUND .....	1
1.2. COMMERCIALY AVAILABLE TECHNOLOGIES .....	2
1.2.1. Air Vented Dryers.....	3
1.2.2. Condenser Tumble Dryers.....	5
1.3. LITERATURE SURVEY .....	8
1.4. EUROPEAN EFFICIENCY REQUIREMENTS .....	13
2. MODELLING.....	16
3. CONDENSER TESTING UNIT .....	22
3.1. DESIGN .....	22
3.2. COMPONENTS OF THE TESTING UNIT .....	25
3.3. CONTROLLING UNIT AND TESTING PROCEDURE.....	28
3.3.1. Controlling Unit.....	28
3.3.2. Testing Procedure .....	29
4. EXPERIMENTS .....	35
4.1. DESIGN OF EXPERIMENT.....	35
4.1.1. Data Analysis .....	35
4.1.2. Design of experiment Parameters .....	37

4.2. EXISTING CONDENSER .....	40
4.2.1. Properties .....	40
4.4.2. Condensation Rate Test Results.....	44
4.4.3. Condenser Efficiency Test Results .....	48
5. DESIGN OF THE NEW CONDENSER.....	52
5.1. CONSTRAINTS .....	52
5.2. DESIGN OF THE PROCESS PASSES.....	53
5.3. DESIGN OF THE COOLING PASSES .....	56
5.4. TEST RESULTS.....	61
5.4.1. Condensation Rate Test Results.....	62
5.4.2. Condenser Efficiency Test Results .....	66
6. EXPERIMENTS ON A TUMBLE DRYER .....	70
7. CONCLUSION AND FUTURE WORK .....	73
7.1. CONCLUSION.....	73
7.1. FUTURE WORK.....	74
APPENDIX A: COMPONENT SPECIFICATIONS .....	75
REFERENCES .....	76
REFERENCES NOT CITED .....	78

## LIST OF FIGURES

Figure 1.1. Evolution of methods to extract water mechanically .....	1
Figure 1.2. Tumble dryer sales (EU27 excluding Baltic countries) .....	3
Figure 1.3. Air vented dryer.....	3
Figure 1.4. Thermodynamic process of an air vented dryer .....	4
Figure 1.5. Heat pump dryer .....	6
Figure 1.6. Air condenser dryer .....	7
Figure 1.7. Thermodynamic process of an air condenser dryer.....	8
Figure 1.8. Improvement over air vented dryer .....	10
Figure 1.9. Effect of tightening components on energy consumption.....	11
Figure 1.10. Energy consumption after tightening the outer tumble dryer cover.....	12
Figure 2.1. Temperature change of process air during a drying cycle.....	16
Figure 2.2. Effect of condenser efficiency on energy consumption .....	20
Figure 2.3. Effect of condenser efficiency for different water collection efficiencies	21
Figure 3.1. Condenser testing unit.....	23
Figure 3.2. Condenser test section.....	24



Figure 3.3. 3D model of the condenser testing unit.....	25
Figure 3.4. Condenser testing unit.....	26
Figure 3.5. Temperature and humidity probes.....	26
Figure 3.6. Annubars and differential pressure sensors.....	27
Figure 3.7. Heater .....	27
Figure 3.8. Humidifier Unit .....	28
Figure 3.9. Control unit.....	29
Figure 3.10. Human machine interface (HMI) of the testing unit .....	30
Figure 3.11. The increase of process air temperature .....	31
Figure 3.12. Condenser testing unit under steady state conditions.....	32
Figure 3.13. Measuring condensation rate.....	32
Figure 3.14. Temperature graph .....	33
Figure 3.15. Relative humidity graph .....	33
Figure 3.16. Volumetric flow rate graph .....	34
Figure 4.1. Control volume for condenser process channels.....	36
Figure 4.2. The existing condenser .....	41
Figure 4.3. Different fin geometries .....	42

Figure 4.4. Strip fin geometry of existing condenser .....	43
Figure 4.5. Fin dimensions of the existing condenser .....	43
Figure 4.6. GLM results of the existing condenser.....	45
Figure 4.7. Effects of quantitative factors.....	46
Figure 4.8. Effect of process channel geometry on condensation rate .....	47
Figure 4.9. Effect ratios of factors on condensation rate .....	48
Figure 4.10. GLM results for condenser efficiency.....	50
Figure 4.11. Effects of quantitative factors on condenser efficiency .....	50
Figure 4.12. Effect of the process channel geometry on the condenser efficiency .....	51
Figure 4.13. Effect ratios of factors on condenser efficiency.....	51
Figure 5.1. Outer dimensions of the condenser .....	52
Figure 5.2. Film condensation .....	53
Figure 5.3. The growth of condensate film thickness.....	54
Figure 5.4. The change of local Nusselt number .....	55
Figure 5.5. Model for fin geometry .....	57
Figure 5.6. Effect of fin width .....	59
Figure 5.7. Effect of fin length .....	60

Figure 5.8. Effect of fin height .....	61
Figure 5.9. The installation of the condenser.....	62
Figure 5.10. GLM results of the new condenser.....	64
Figure 5.11. Effect of factors on condensation rate.....	65
Figure 5.12. Effect ratio of factors on condensation rate.....	65
Figure 5.13. GLM analysis of the efficiency for the new condenser.....	67
Figure 5.14. Effect of quantitative factors on condenser efficiency.....	68
Figure 5.15. Effect of cooling air channel geometry.....	68
Figure 5.16. Effect ratio of factors and their interactions on condenser efficiency.....	69
Figure 6.1. Three process pass condenser.....	70
Figure 6.2. Water collecting efficiency test results .....	71
Figure 6.3. Specific energy consumption test results .....	72

## LIST OF TABLES

Table 1.1. Sales distribution by air technology .....	5
Table 1.2. Sales distribution of heat pump dryers .....	6
Table 1.3. EU energy label according to EN 61121:2005 .....	14
Table 2.1. Input parameters and variables .....	19
Table 4.1 Factors of the DOE .....	37
Table 4.2. Factor levels of the DOE .....	39
Table 4.3. DOE with 20 test runs.....	40
Table 4.4. Dimensions of process passes.....	41
Table 4.5. Dimensions of cooling passes .....	42
Table 4.6. The condensation rate results .....	44
Table 4.7. Condenser efficiency results.....	49
Table 5.1. Dimensions of the process passes.....	56
Table 5.2. Dimensions of the cooling passes.....	56
Table 5.3. Fin dimensions of the new condenser.....	60
Table 5.4. Condensation rate results of the new condenser) .....	63

Table 5.5. Condenser efficiency results of the new condenser.....	66
Table A.1. Insulation material .....	75
Table A.2. Temperature and humidity probes .....	75
Table A.3. Differential pressure sensors.....	75

## LIST OF SYMBOLS

$A_C$	Corrected area
$A_{CROSS}$	Cross section area of a pass
$c$	Cooling
$C_{p_{AIR}}$	Specific heat capacity of air
$C_{p_i}$	Specific heat capacities of a dryer components
$\dot{E}_{cond}$	Latent heat taken from the process per second
$E_{cond}$	Energy required to evaporate the water which is then captured in the condenser
$\dot{E}_{cool}$	Heat transferred to the cooling air per second
$E_{cool}$	Energy removed from the process air
$E_{dryer}$	Energy needed for the dryer mass to reach its equilibrium temperature
$E_{LABEL}$	Energy consumption of a tumble dryer according to the EN 61121:2005
$E_{leakage}$	Energy needed for vaporizing the leakage water
$E_{load}$	Energy needed for heating the load to equilibrium temperature
$E_{losses}$	Thermal losses from the chassis of the dryer
$E_{motor}$	Energy spent by the motor to drive the tumble and the fans
$E_{TOTAL}$	Measured energy consumption of a tumble dryer
$f$	fin
$H$	Height of a pass
$h$	Convection heat transfer coefficient
$h_{fg}$	Enthalpy change of vaporization for water
$h_g$	Enthalpy of water vapor
$k$	Thermal conductivity
$L$	Length of a pass
$L_C$	Corrected length
$\dot{m}_{air}$	Mass flow rate of air
$m_i$	Mass of dryer components

$m_{laundry}$		Rated capacity of the tumble dryer
$m_{laundry_0}$		Conditioned mass of the laundry
$m_{tank}$		Condensate collected in the tank
$\dot{m}_{water}$		Condensation rate
$m_{water_i}$	I	initial water mass on the laundry
$m_{water_f}$		Final water mass on the laundry
N		Number of passes
$Nu$		Nusselt number
P		Pressure
$P$		Perimeter
p		Process
$Pr$		Prandtl number
Q		Volumetric flow rate
Re		Reynolds number
$RH$		relative humidity
T		Temperature
$t$		Fin thickness
$T_{IN}$		Air condenser inlet temperature
$T_{OUT}$		Air condenser outlet temperature
$T_{eq}$		Equilibrium temperature
$V$		Velocity
W		Width of a pass
$w_{IN}$		Air condenser inlet specific humidity
$x$		Distance from the inlet of a channel
$\Delta h_f$		Enthalpy change of water
$\delta$		Condensate thickness
$\eta$		Condenser efficiency
$\eta_{col}$		Water collecting efficiency
$\eta_f$		Fin efficiency
$\theta$		Declination angle

$\mu_f$	Final actual moisture content of the laundry
$\mu_{f0}$	Final nominal moisture content of the laundry
$\mu_i$	Initial actual moisture content of the laundry
$\mu_{i0}$	Initial nominal moisture content of the laundry
$\nu$	Kinematic viscosity
DOE	Design of experiment
EU	European Union
GLM	General linear model
HMI	Human machine interface



# 1. INTRODUCTION

## 1.1. BACKGROUND

Since the beginning of the civilization, washing and drying of laundry has become a daily routine of human life. For centuries hands and the sun had been the only recourse for washing and drying the clothes and that's why cleaning the laundry had been a very labor and time intensive process.

After the washing process in all the applications commonly used for drying water have been extracted from clothes in two ways:

- Mechanically
- Thermally

Until the beginning of the 19th century wringing clothes by hand had been the only mechanical way for extracting the water from the clothes. After the invention of the mangle machine, the first known clothes wringer added to the washing machine was seen in 1861. From the beginning of the 1930s, centrifugal forces by spinning were employed to extract water from clothes. Thanks to the introduction of the two-speed motors, the rotating speed during spinning could be increased. Figure 1.1. shows the evolution of mechanical methods to extract water. Washing machines with spinning cycles, which is commonly used today, provide the latest mechanical method for extracting water.



Figure 1.1. Evolution of methods to extract water mechanically

The first and even today most commonly used thermal method for extracting water from laundry is to dry under the sun. In the early 1800s, clothes dryers were first being invented in England and France. One common kind of early clothes dryers was the ventilator, and the first one is known to be built by a Frenchman named Pochon. The ventilator was a barrel-shaped metal drum with holes in it and it was turned by hand over a fire. In 1892 an early American patent for a ventilator type clothes dryer, which used stove as heat source, was granted to George T. Sampson. In 1915 the first electrical drying machine was invented. Thanks to subsequent improvements, tumble dryers has now become most popular, in which textile material is tumbled in a rotating drum and dried by heated air passing through.

## **1.2. COMMERCIALY AVAILABLE TECHNOLOGIES**

As a result of the changing consuming habits and understanding of cleaning, the demand for clean clothes increases more and more every day. This situation not only expands the demand for textile products but also makes people wash more clothes more frequently. White appliance companies try to facilitate their consumers' life by producing washing machines with higher capacities, shorter washing programs and faster spinning cycles but the need for drying the washed clothes thermally still exists.

The newly built apartments with no appropriate space like balcony and the time required to dry clothes by hanging causes more people to buy tumble dryers every day. As seen in Figure 1.2, the global European market of tumble dryers is increasing. Between 2002 and 2007, sales have globally increased by 14 per cent and it is estimated that 21.1 million tumble dryers will be sold in EU between 2010 and 2015, which means a sale of 4.2 million dryers on average every year.

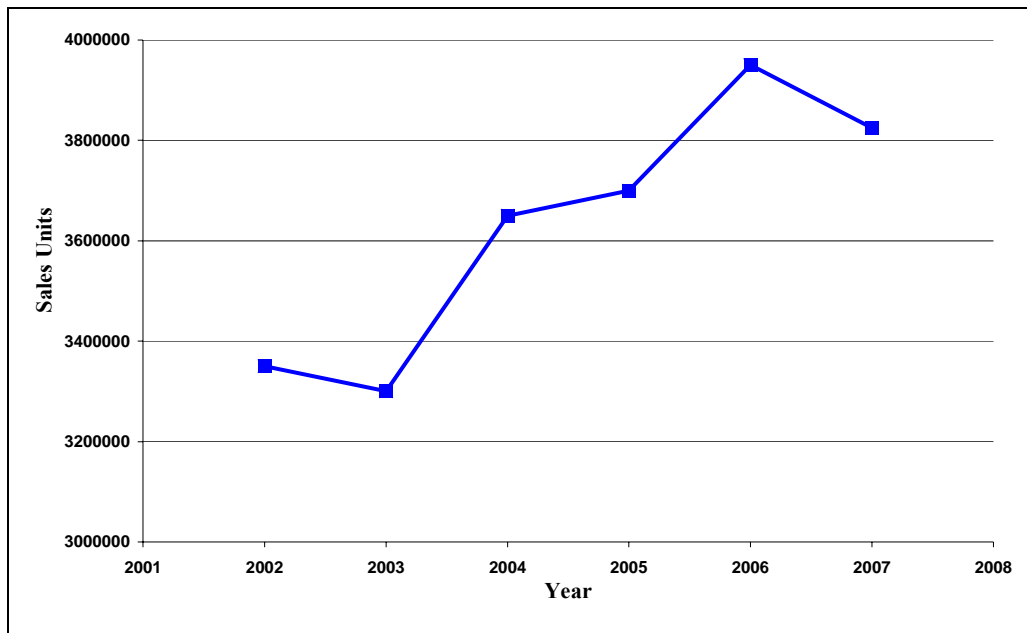


Figure 1.2. Tumble dryer sales (EU27 excluding Baltic countries)

Today there are two main types in tumble dryers:

- Air vented tumble dryers
- Condenser tumble dryers

### 1.2.1. Air Vented Dryers

As shown below in Figure 1.3, a conventional air vented dryer consists of a drum (for clothes), a fan, a heater (using a resistive heating part or combusting some type of fuel such as natural gas), a motor to rotate the drum and some ducts to exhaust the moist air to the outside.

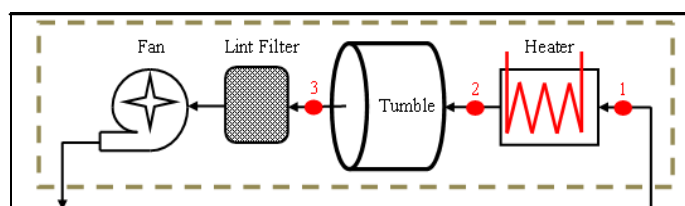


Figure 1.3. Air vented dryer

In air vented tumble dryers room air is sucked by a fan through the heater (1-2). The heated air then enters the clothes drum, is brought into contact with damp clothing and facilitates the evaporation of liquid water from the textiles (2-3). After leaving the drum the humid air passes through a lint filter and is evacuated outside by the fan through a flexible pipe.

As shown on the psychrometric chart in Figure 1.4, heating the room air increases the driving potential for the evaporation process of the moisture in the clothes. The humidification process within the tumble is essentially an isenthalpic process where the energy needed for evaporation is supplied by energy carried by the heated air.

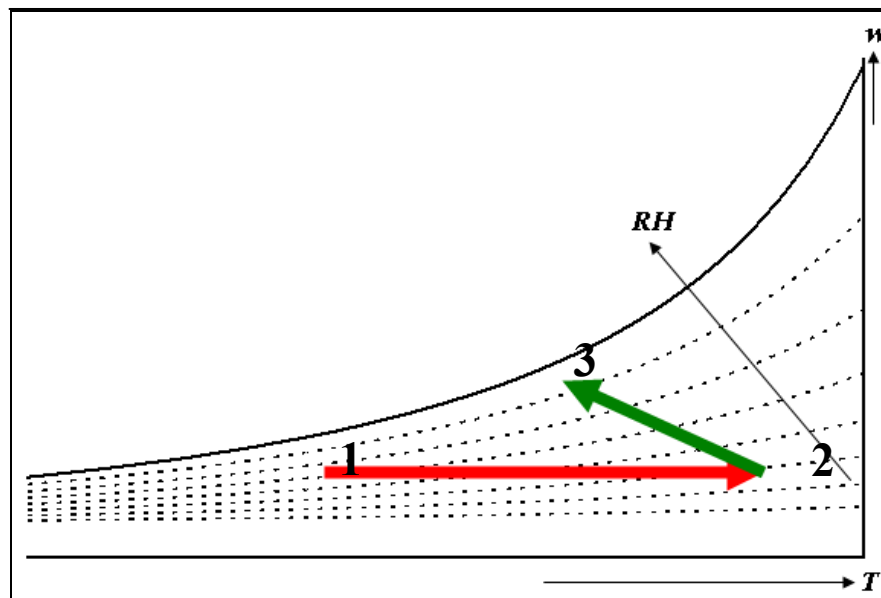


Figure 1.4. Thermodynamic process of an air vented dryer

The conventional process of air vented dryer is simple, effective, reliable and relatively fast. However, it has the disadvantage of requiring a duct to exhaust the air to the outdoors and this also causes inefficiency because especially in cold climates household heating system must compensate for the exhausted air by additional heating. In order to reduce the heating costs a condenser can be installed between the hot exhaust air and incoming room ambient air but this time the system itself would be more costly and would still require an external ducting.

### 1.2.2. Condenser Tumble Dryers

Instead of exhausting the humid air outside, a condenser tumble dryer uses a heat exchanger (namely, a condenser) where vapor in the humid air condenses into water that is collected into either a drain pipe or a collection tank. This system is of a closed cycle and does not require a venting duct to the exterior of the house. Therefore, consumers may place the dryer virtually at any location within their house. Today two types of condenser tumble dryers can be found on the market:

- Heat pump dryers
- Air condenser dryers

Although air vented dryers are very prevalently used in U.S. and Canada, their market share is dropping in Europe. As seen from Table 1.1, in Eastern Europe, condenser tumble dryers have already began to dominate the market such that they took over 75 per cent of the sales in 2005 [1].

Table 1.1. Sales distribution by air technology

Technology	Western Europe		Eastern Europe	
	per cent		per cent	
	2002	2005	2002	2005
<b>Air Vented</b>	51.4	45	33.9	24.2
<b>Condenser</b>	48.6	55	61.9	75.3
<b>Unknown</b>	0	0	4.2	0.5

#### 1.2.2.1. Heat Pump Dryers

The heat pump dryer is relatively a new concept in the dryer market. The first heat pump dryer was introduced in 1997 by Electrolux. As shown in Table 1.2, heat pump dryers have not been able to grab a large market share in Europe [1].

Table 1.2. Sales distribution of heat pump dryers

Region	Western Europe		Eastern Europe	
Year	2002	2005	2002	2005
Market Share (per cent)	0.4	0.5	0.1	0.5

As it can be seen from Figure 1.5, a conventional heat pump dryer basically consists of a drum, filter and fan within the process cycle; a condenser, evaporator, expansion valve and compressor within the cooling cycle.

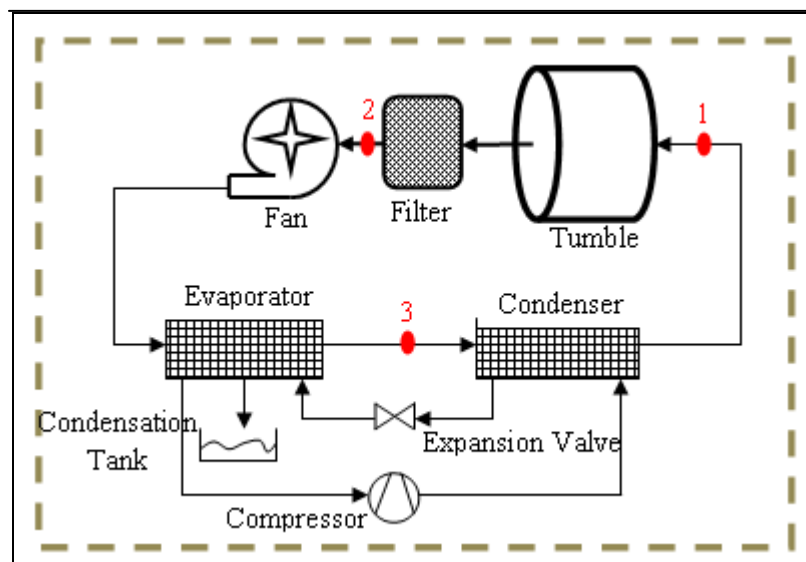


Figure 1.5. Heat pump dryer

In heat pump dryers, after passing through the tumble and the filter (1-2), humidified air is blown to the evaporator where its temperature is reduced below the dew point and condensation occurs (2-3). After the evaporator, the process air goes through the condenser where it is heated before being blown back to the tumble (3-1).

Thanks to the heat recovery system provided by the cooling cycle, heat pump dryers consume much less energy than the other technologies in the market. Because of the high prices based on the high manufacturing costs, however, its market share as of now could not reach even 1 per cent.

### 1.2.2.2. Air Condenser Dryers

Thanks to the improvements in the condensing technology, the air condenser tumble dryers began to dominate the European market while they are not still popular in United States. Table 1.1. shows that in Eastern Europe air condenser dryers already took more than 75 per cent of the sales with a significant increase of 13.4 per cent market share in number of sales between 2002 and 2005 [1].

As shown in Figure 1.6. below, an air condenser dryer consists of a heater, drum, filter, fan and condenser in the closed process cycle and also a secondary fan in the cooling cycle.

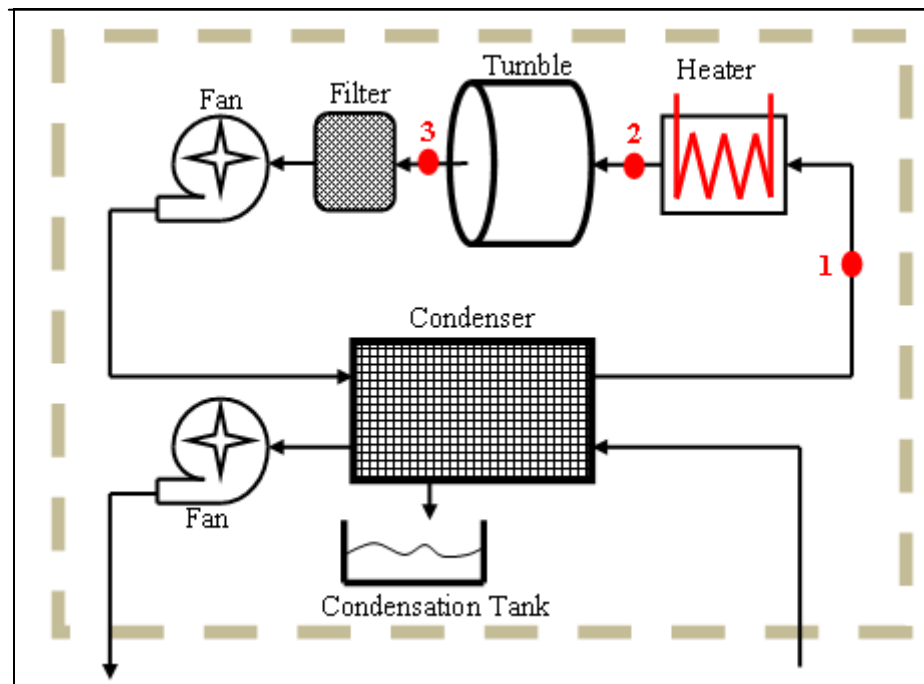


Figure 1.6. Air condenser dryer

The process air is heated up by a heater before entering the tumble. As a result, its relative humidity decreases, and thus the evaporating potential of the process air increases (1-2) as shown on the psychrometric chart in Figure 1.7. In the tumble, the hot and dry air evaporates the moisture from the clothes (2-3). The humid process air that exits the tumble is blown to the condenser by a process fan after passing through the filter. In the condenser the humid process air is cooled by the ambient air which is blown by another fan (3-1),

resulting in the condensation of the water vapor in the process air. The condensed water is either pumped to a holding tank for manual removal or directly pumped to drain so that users may not have to periodically empty the large condensate holding tank.

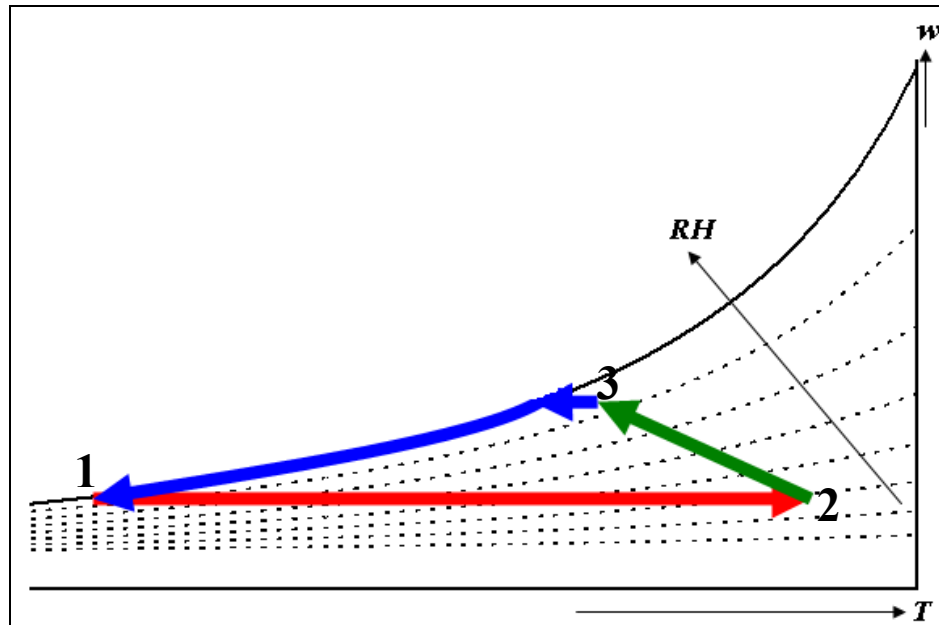


Figure 1.7. Thermodynamic process of an air condenser dryer

Despite the disadvantages of being costly and requiring more regular maintenance such as manual water drainage and the removal of lint accumulated in the condenser, air condenser dryers have become a method more favored for automated drying in the EU. In today's world where energy resources are dropping at alarming rates due to the massive global demand, every little step toward improvement should be considered important for these huge energy consuming home appliances.

### 1.3. LITERATURE SURVEY

Unfortunately the number of studies related to the tumble dryers is very limited in the open literature. In one of the earliest studies Hekmat and Fisk investigated four different energy saving techniques which are reducing the air flow rate, recirculation of exhaust air, heat recovery by utilizing an air-to-air heat exchanger, and finally recirculation process air and using heat pump for condensation [2]. It was found that, in comparison



with the baseline performance, eight per cent energy could be saved by matching air flow rate and heater input to the size of the dryer load. This matching could be obtained with a variable electric heater and a multiple speed motor for the fan. Recirculation of exhaust air resulted in a 10-18 per cent decrease in energy consumption, depending on the recirculation ratio. A 26 per cent reduction in energy consumption was achieved with heat recovery by utilizing an air-to-air heat exchanger in the preheating mode. Finally tests were performed using a heat pump and a residential dehumidifier was coupled to a clothes dryer. This integration resulted again in a closed system with 100 per cent heat recovery and tests showed a 33 per cent reduction in energy consumption.

In 1997 Conde discussed the existing tumbler dryer technology and its shortcomings in his study [3]. He has shown that conventional condensation and recirculation tumblers though solving some other problem, in fact increase the specific energy consumption. Based on the measurements on a small commercial open loop tumbler dryer, it is demonstrated that the use of heat recovery heat exchangers improves the energetic efficiency of the drying process. According to the tests he verified that the optimal size of the heat exchanger which is used for heat recovery does not depend much upon the kind of textile load, but essentially on the specific air flow rate. His study also showed that loads lower than nominal decrease the drying efficiency. In 1997 Kao also tested the conventional air vented and condenser dryers following the U.S. Department of Energy (DOE) test procedure [4]. He found that for air condenser dryers energy required to dry one kg of moisture is bigger than for air vented dryers. In this study the maximum effect of room humidity to clothes dryer energy consumption was to be found 0.79 per cent for each 10 per cent relative humidity change.

In their study Bansal, Braun and Groll discussed the drying processes of four different designs of household clothes tumbler dryer that are air vented dryer, air vented dryer with heat exchanger (open cycle), air condenser dryer (closed cycle) and air condenser dryer with additional heat exchanger for heat recovery [5]. Simple simulation models were developed for each dryer type using the Engineering Equation Solver (EES) software package. The ambient air was assumed to be at 20°C and 60 per cent relative humidity except for the air vented dryer where the relative humidity was a variable. The

main inputs of the models were power needed for the drum, flow rate of air, relative humidity at the tumble exit and heat exchanger effectiveness. The main output was the specific moisture extraction rate (MER), (kWh / weight of wet clothes). According to the given operating conditions as it can be seen from Figure 1.8, the open-cycle condensing dryer and the closed-cycle condensing dryer with heat recovery are significantly more efficient (about 14 per cent) than conventional air vented dryer.

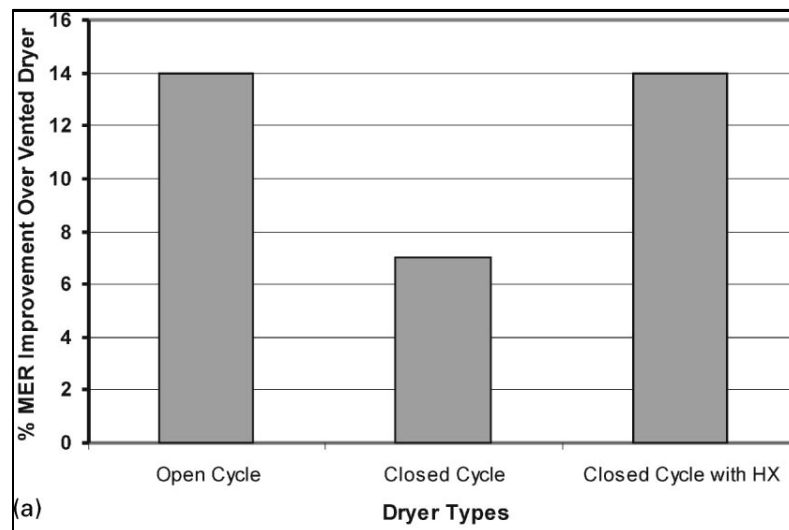


Figure 1.8. Improvement over air vented dryer [5]

In 2003 Bassily and Colver studied on the mass transfer within the tumble and they defined a mass transfer correlation of the Sherwood number with dimensionless numbers based on experimental data [6]. For comparison purposes, a second correlation for the Sherwood number was evaluated experimentally for a single piece of cloth stretched perpendicular to the flow in a pipe and defined as ideal mass transfer process for clothes drying. Results showed that increasing the weight of clothes and tuning drum speed for optimum contact for clothes with the drying agent could enhance the area of mass transfer. Also increasing the inlet air temperature and improving the mixing process inside the drum increases the mass transfer coefficient. Comparing the result of the 32 test runs with the ideal mass transfer process, the dryer mass transfer efficiency was only 26.4 per cent. In 2005 in order to optimize the annual cost of clothes dryers Bassily and Colver developed a correlation for the evaporative mass flux produced in the drum [7]. The cost optimization studies indicated that decreasing the heater power and selecting the optimum values of

parameters for the heater and dryer operation to achieve optimum performance could reduce the drying cost. They also pointed out that drum speed that corresponds to the optimum annual cost decreases as the heater power increases and finally installing an optimum heater and a speed controller for the fan and operating the dryer at the optimum settings could save 37.45 per cent in annual cost.

In 2004 Berghel, Brunzell and Bengtsson carried out a leakage survey for increasing the efficiency of an air condenser dryer [8]. In order to decrease leakage, the internal system was tightened. The back of the drum was tightened with an extra sealing (A). A return tube, transporting condensed moisture from a condensation water container to the water pump, has been sealed (B). The condenser was tightened in both ends to decrease leakage between internal and external flows (C). Finally, the shaft of the fan was tightened with a radial sealing (D). In order to maintain a constant airflow in the internal system test runs with the different tightening options were performed with two different fans, one normal and one large. As shown in Figure 1.9, tightening performed on the internal system of the tumble dryer caused an increase in the energy consumption due to the changes in the process parameters, which leads to a decrease in condenser capacity.

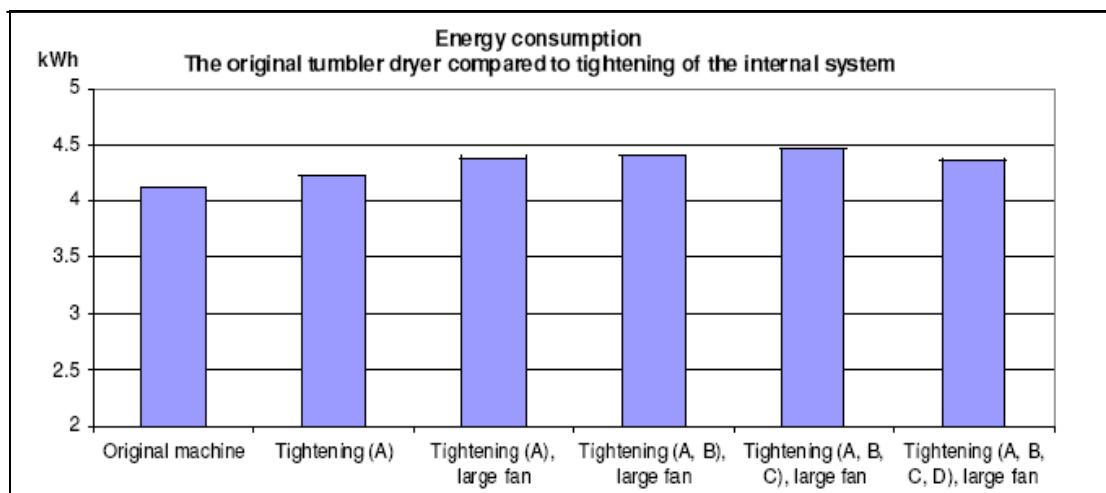


Figure 1.9. Effect of tightening components on energy consumption [8]

After tightening the outer tumble dryer cover, more tests were performed with the load consists of 5.0kg of cotton and 3.5kg of water as ordained by The Swedish Consumer

Agency 1996:3. As it can be seen from Figure 1.10, the energy consumption of the dryer is reduced at about 6.5 – 9 per cent and came closer to the B Class that is shown with dashed line.

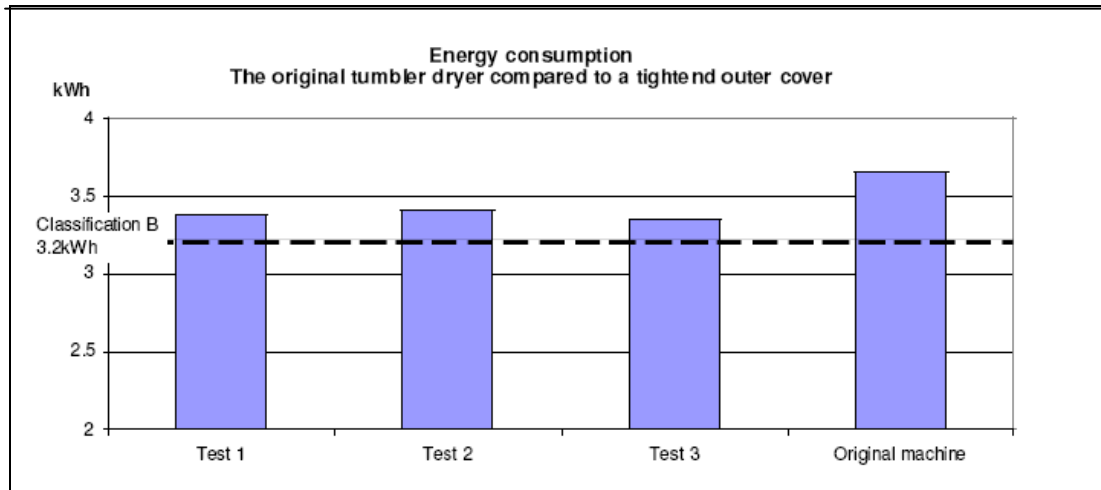


Figure 1.10. Energy consumption after tightening the outer tumble dryer cover [8]

In 2006 Brunzell investigated the effect of the location of the leakage on the performance of the closed cycle dryer [9]. It was found that the leakage between the heater and the drum with high temperature air and a low relative humidity means a considerable loss of energy from the internal system. This study also showed that leakage into the internal system between the drum and the condenser also increases the specific energy use, which is due to larger losses over the condenser if the same amount of water vapor is to be condensed. Finally, it is estimated that the specific energy use is reduced by approximately 17 per cent by insulating the back cover of the dryer, by reducing leakage between the heater and the drum and by opening the internal system during the falling drying rate period.

During the literature survey the only study which focused on the condenser of a closed cycle tumble dryer belonged to Cochran [10]. In his thesis study he replaced the air-air condenser of the dryer with a Surface Tension Element (STE) device. The operation of the STE was compared to that of the typical air-to-air heat exchanger/condenser used in condensing dryers and the results indicated that the STE used an average of 0.616 kilowatt-

hours per kilogram dry laundry while the air-to-air heat exchanger/condenser used an average of 0.643 kWh/kg. An analytical model was also constructed that well predicted the operation of the STE under steady state conditions.

In conclusion, the number of studies in concern with the air condenser dryers is very limited and unfortunately none of them address the air-air condenser for reducing the energy consumption. Differing from the researches mentioned above, the object of the present study which will be mentioned below is to reduce the energy consumption of an air condenser dryer by increasing the efficiency of the condenser.

#### **1.4. EUROPEAN EFFICIENCY REQUIREMENTS**

Owing to the significant dropping in the energy resources, in today's world energy becomes more important than ever. This situation also affects the standardization of the tumble dryers which consume huge amount of energy compared to the other home appliances. Today the valid standard within The EU is EN 61121:2005. This standard defines the test methods for measuring performance of tumble dryers and also represents the basis of the current European energy labeling system. As a result of the increasing importance of energy, labeling formed for the tumble dryer is very forceful. Today there is still no conventional air condenser dryer on the market that could succeed in obtaining A energy labeling. For air vented tumble dryers the situation is also the same and unfortunately there is no existing conventional air vented dryer which could reach A on the energy labeling shown on Table 1.3.

Table 1.3. EU energy label according to EN 61121:2005

<b>EU Energy Label</b>	<b>Condensing Dryer Energy Consumption (kWh/kg)</b>	<b>Air-Vented Dryer Energy Consumption (kWh/kg)</b>
A	EC ≤ 0.55	EC ≤ 0.51
B	0.55 < EC ≤ 0.64	0.51 < EC ≤ 0.59
C	0.64 < EC ≤ 0.73	0.59 < EC ≤ 0.67
D	0.73 < EC ≤ 0.82	0.67 < EC ≤ 0.75
E	0.82 < EC ≤ 0.91	0.75 < EC ≤ 0.83
F	0.91 < EC ≤ 1.00	0.83 < EC ≤ 0.91
G	EC > 1.00	EC > 0.91

According to the EN 61121:2005, total energy consumption of a tumble dryer ( $E_{LABEL}$ ) that can be declared by the manufacturer on the product label is calculated by testing a defined cotton laundry that is wetted with water under defined conditions. The declared energy consumption of the laundry depends on the measured energy consumption, the ratio of the nominal moisture content to actual one and also the ratio of the rated capacity of the program to the conditioned mass of the laundry.

$$E_{LABEL} = E_{TOTAL} \cdot \frac{1.14(\mu_{i0} - \mu_{f0}) m_{laundry}}{(\mu_i - \mu_f) m_{laundry_0}} \quad (1.1.)$$

The nominal moisture contents of the laundry are 60 per cent for initial ( $\mu_{i0}$ ) and zero per cent for the final ( $\mu_{f0}$ ) case. The actual moisture contents are calculated by the formulas given below.

For initial actual moisture content;

$$\mu_i = \frac{m_{water_i}}{m_{laundry}} \quad (1.2.)$$

For final actual moisture content;

$$\mu_f = \frac{m_{water_f}}{m_{laundry}} \quad (1.3.)$$

## 2. MODELING

In order to understand the effect of the condenser on the energy consumption of a tumble dryer which has huge energy consumption values comparing to other home appliances, it is very important to model the energy needed for drying a certain amount of laundry with an air condenser tumble dryer. As seen in Figure 2.1. which shows the temperature change of the process air during a drying cycle, the drying process can be divided into three main phases: heating phase, equilibrium phase and ventilating phase.

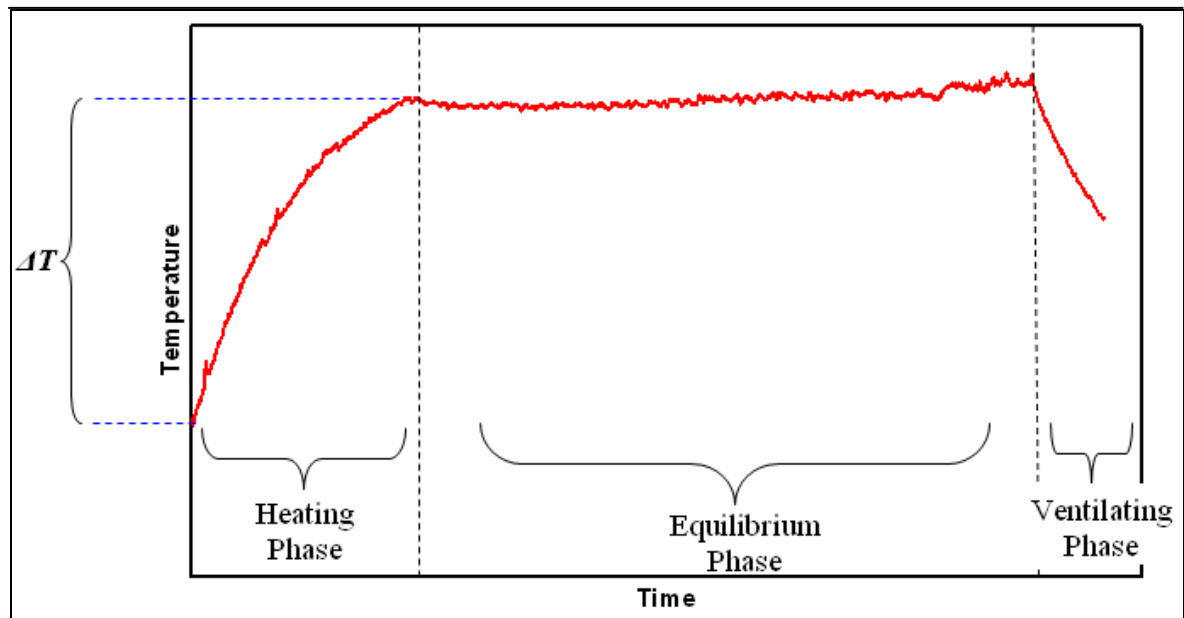


Figure 2.1. Temperature change of process air during a drying cycle

Energy needed ( $E_{dryer}$ ) for the dryer mass to reach its equilibrium temperature ( $T_{eq}$ ) can be calculated from the sum of the energy that every component ( $i$ ) stores until they reach their equilibrium temperature. Accordingly, as given in the following formula, every component's mass ( $m_i$ ) is multiplied with their specific heat capacities ( $C_{p_i}$ ) and the temperature increase ( $\Delta T$ ). The sum of the results gives the total energy needed for a tumble dryer to reach its equilibrium temperature.



$$E_{dryer} = \sum_{i=1}^n m_i C_{pi} \cdot \Delta T \quad (2.1.)$$

During the heating phase, the conditioned laundry ( $m_{laundry}$ ) and also the initial water within the laundry ( $m_{water_i}$ ) have to be heated in addition to the energy needed for heating the dryer mass. Similarly, by using the laundry's specific heat capacity values and the water's enthalpy change ( $\Delta h_f$ ), the energy needed for heating the load ( $E_{load}$ ) can be calculated as:

$$E_{load} = m_{laundry} \cdot C_{p_{laundry}} \cdot \Delta T + m_{water_i} \cdot \Delta h_f \quad (2.2.)$$

As mentioned in the previous chapter, for air condenser tumble dryers in which the process air should flow in a closed cycle through the tumble, condenser and the heater, there may be some leakage problems according to the production or working conditions. As a result, all of the water within the laundry which is vaporized in the tumble is not condensed within the condenser and some of this water vapor escapes to the surrounding. In order to address the leakage problem of a dryer, therefore, water collecting efficiency ( $\eta_{col}$ ) is calculated by dividing the amount of water condensed within the condenser and collected in the tank ( $m_{tank}$ ) by the total water mass within the laundry ( $m_{water_i}$ ).

$$\eta_{col} = \frac{m_{tank}}{m_{water_i}} \quad (2.3.)$$

In order to calculate the energy needed for evaporating the water within the laundry, the water vapor which is dispersed to the surrounding due to the leakage problems and the water vapor which is collected by the condenser should be taken into account separately. The energy needed for vaporizing the leakage water ( $E_{leakage}$ ) can simply be calculated by using the enthalpy change of vaporization for water ( $h_{fg}$ ) in the formula given below.

$$E_{leakage} = (1 - \eta_{col}) \cdot m_{water} \cdot h_{fg} \quad (2.4.)$$

In an ideal drying system where there are no existing thermal losses within the condenser and where the process air flows into the condenser with 100 per cent relative humidity, the energy required to evaporate the water which is then captured in the condenser can be calculated as follows:

$$E_{cond} = \eta_{col} \cdot m_{water} \cdot h_{fg} \quad (2.5.)$$

Under the real working conditions, the energy needed to vaporize the water which is collected by the condenser is equal to the energy that is removed from the process air ( $E_{cool}$ ). Since the process air does not flow into condenser with 100 per cent relative humidity, some of the energy that is transferred to the cooling air is sensible heat and is not useful for condensation. Hence, the removed process energy has to be regained from the heater and can be calculated by integrating the enthalpy change of process air within the condenser for the whole drying cycle.

$$E_{cool} = \int \dot{m}_{air} \left( (c_{p_{AIR}} \cdot T_{IN} + w_{IN} \cdot h_{g_{IN}}) - (c_{p_{AIR}} \cdot T_{OUT} + w_{OUT} \cdot h_{g_{OUT}}) \right) dt \quad (2.6.)$$

The ratio of the  $E_{cond}$  to the  $E_{cool}$  is an indicator of efficiency ( $\eta$ ) for a condenser. A condenser with high efficiency holds the sensible heat losses of the process air to minimum and leads to higher condensation rates, resulting in less energy consumption and shorter drying cycle.

$$\eta = \frac{E_{cond}}{E_{cool}} \quad (2.7.)$$

In addition to the energy needed for heating up the whole system to the equilibrium temperature during the heating phase and the energy needed to vaporize the water from the laundry during the whole cycle, the thermal losses from the chassis of the dryer to the surrounding ( $E_{losses}$ ) and also the energy spent by the motor to drive the tumble and the fans ( $E_{motor}$ ) should be taken into account. Therefore, the total energy consumption of a dryer per a kg of laundry ( $E_{TOTAL}$ ) can be determined by the formula given below.

$$E_{TOTAL} = \frac{(E_{dryer} + E_{load} + E_{leakage} + E_{cool} + E_{motor} + E_{losses})}{m_{laundry}} \quad (2.8.)$$

The energy consumption of a dryer has been calculated by the formulas given above. The input parameters and variables that have been used in the calculation are listed in Table 2.1.

Table 2.1. Input parameters and variables

Rated capacity and conditioned mass of the laundry (kg)	7
Total operation period (min)	130
Heat capacity of the laundry (kJ/kg°C)	1.3
Temperature increase of the laundry and the process air (°C)	45
Mass of the initial water on the laundry (kg)	4.2
Final actual moisture content of the laundry (%)	0
Mass of the dryer (kg)	38
Average of the heat capacities of the dryer's components (kJ/kg°C)	0.5
Average of the temperature increase of the dryer's components (°C)	35
Motor power (kW)	0.2
Expected heat loss (kWh)	0.3
Water collecting efficiency (%)	70

With the given input parameters and variables, the energy consumption is calculated with the formulas given above and presented in Figure 2.2. in terms of EN 61121 energy labeling ( $E_{LABEL}$ ). As shown in the figure, the energy consumption is directly affected by the condenser efficiency. By increasing the condenser efficiency from 70 per cent to 100 per cent, the energy consumption can be decreased from 0.78 to 0.647 kWh/kg. This means a 17 per cent improvement in the energy consumption and a switch from energy class D to C.

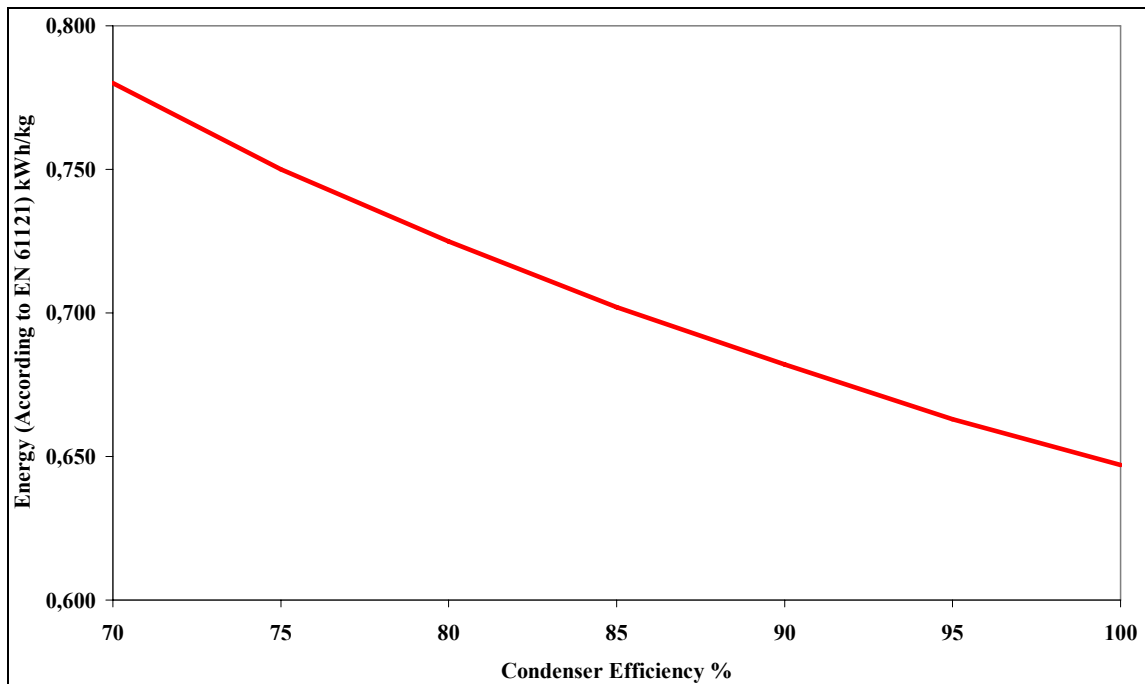


Figure 2.2. Effect of condenser efficiency on energy consumption

The water collection efficiency of a condenser tumble dryer is also considered as important as the energy consumption and the customers begin to prefer the dryers that give off less humid air to the surrounding. Consequently, the use of the water collection efficiency for labeling the condenser dryers is on the agenda of European Committee of Domestic Equipment Manufacturers (CECED) and manufacturers try to minimize the leakage problems to obtain higher water collection efficiency values in the labeling. These improvements on the water collection efficiency unfortunately affect the energy consumption values in a negative way. Figure 2.3. shows the energy consumption of a dryer with different water collection efficiencies. It is apparent that the condenser efficiency becomes much more important for dryers that have higher water collection efficiencies. For a dryer with 90 per cent water collection efficiency, the increase of the condenser efficiency from 70 to 100 per cent results in the reduction of the energy consumption from 0.818 to 0.647 kWh/kg which means a 21 per cent improvement in the energy consumption.

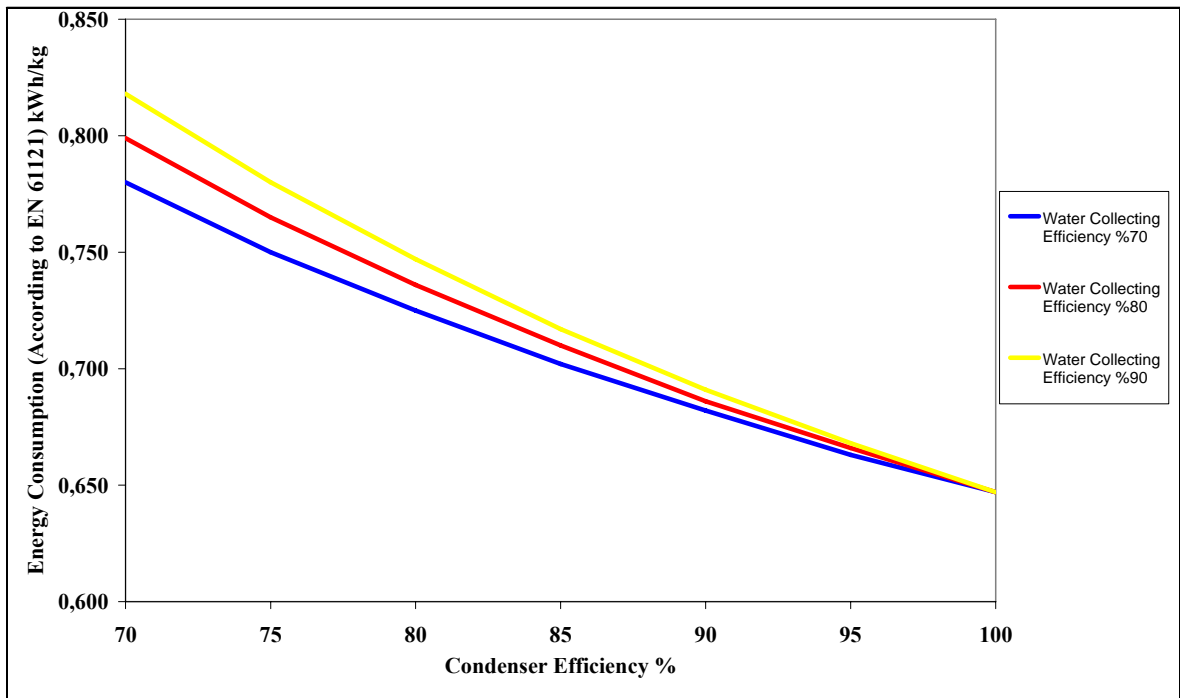


Figure 2.3. Effect of condenser efficiency for different water collection efficiencies

### **3. CONDENSER TESTING UNIT**

In the project, noting the importance of condenser efficiency on energy consumption of an air condenser dryer, a condenser testing unit has been set up to examine the performance of condensers on different working conditions. The condenser testing unit intends to determine the optimum working conditions of existing tumble dryer condensers and to compare the performance of new condenser designs with the existing ones.

#### **3.1. DESIGN**

The studies on condenser testing unit have been started with designing. For the purpose of simulating an air condenser dryer, a testing unit that has a closed process cycle and an open cooling cycle was designed. Similar to the air condenser dryers, a heater to heat the process air is embedded into the process channel, and a humidifier unit is installed into the process channel right after the heater for the purpose of simulating the vaporization process in the tumble of an actual air condenser dryer. Heated and humidified air is directed first to the condenser and then back to the heater. In order to discharge the condensate out of the system, a small hole is placed at the bottom of the channel after the exit of the condenser.

The cooling channel design is also based on the air condenser dryer. As shown in Figure 3.1, the cooling channel system is an open cycle where the ambient air is sucked into the condenser with the help of a fan. After cooling the process air within the condenser, the cooling air flows out back to the ambient.

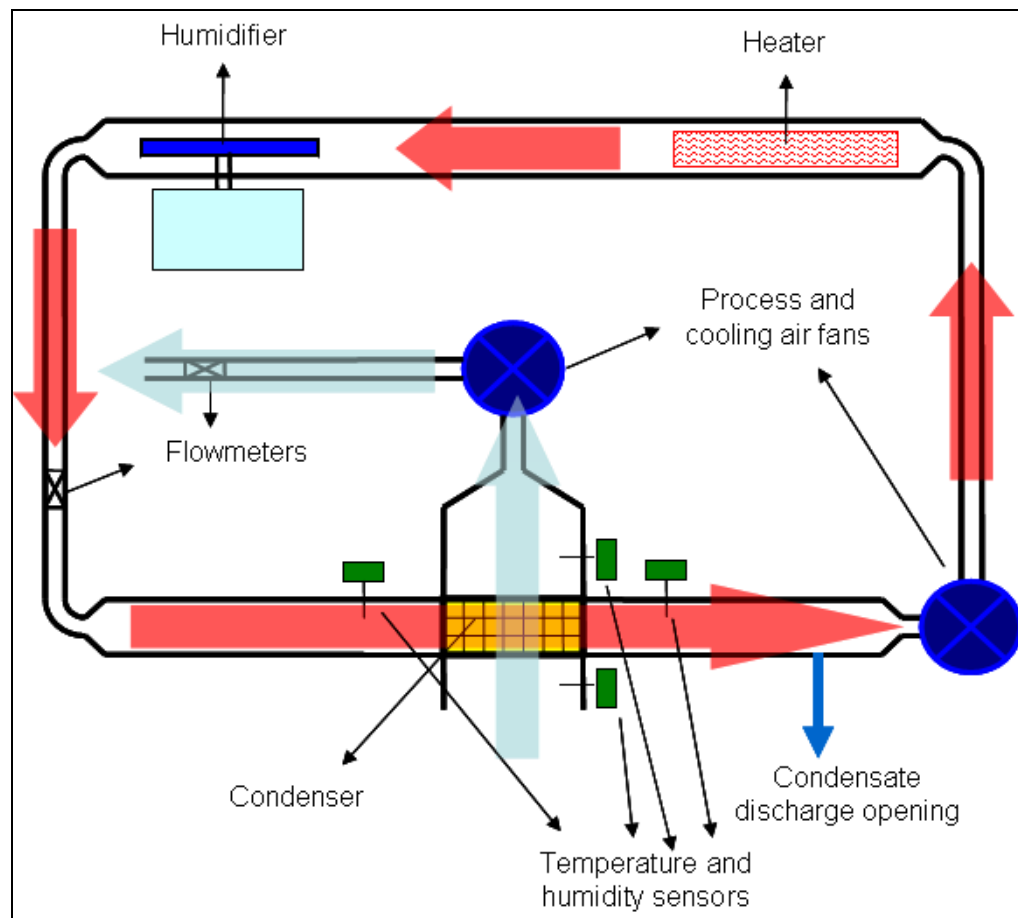


Figure 3.1. Condenser testing unit

Temperature and humidity sensors were installed at the inlets and outlets of the condenser for both process and cooling channels. Also the volumetric flow rates of both process and cooling channels were measured by flow meters. A PLC unit which is run by a SCADA program was employed to establish operating conditions by controlling the heater, humidifier and the fans according to the data received from the sensors mentioned above.

More detailed 3D model has been employed to design the condenser test section of testing unit. The condenser section was designed in such a way that it may accommodate both the benchmark condensers which are used in the present dryers and the condensers that will be designed with different dimensions. In order to investigate the effect of the condenser inlet channel geometries on the condenser performance, inlet guiding areas were formed at the inlets of both process and cooling channels. As it can be seen from Figure

3.2, the guiding plates may be placed in these areas to simulate flows which enter the condenser with  $90^\circ$  turn.

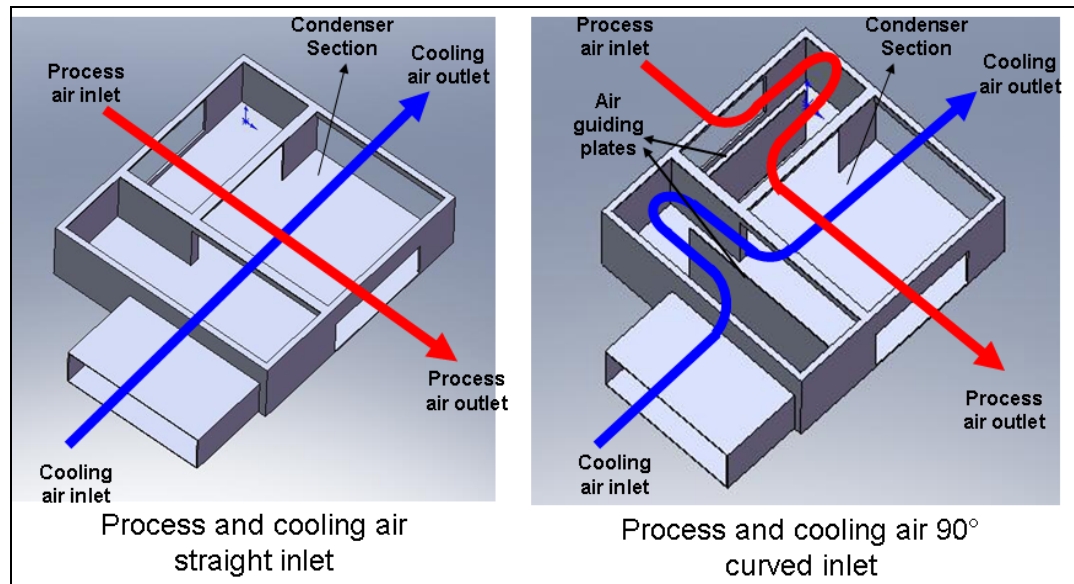


Figure 3.2. Condenser test section

As it can be seen from Figure 3.3, the condenser section was assembled to the channels with a  $3^\circ$  incline in order to discharge the condensate out of the condenser. Also the process channels at the inlet and outlet of the condenser section and the cooling channel at the outlet section were designed with covers that can be opened, so that a series of meshes may be easily placed at these sections to straighten non-uniformities of flows if any.



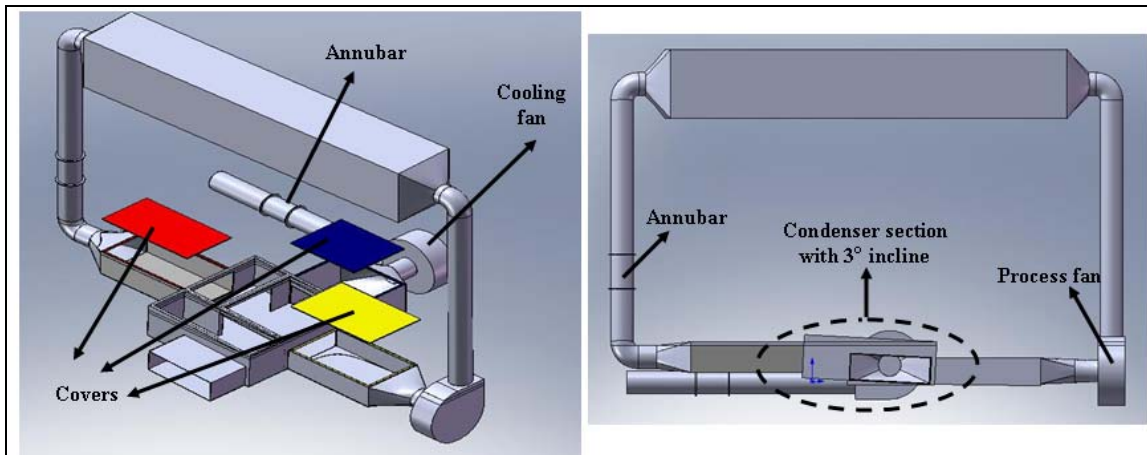


Figure 3.3. 3D model of the condenser testing unit.

### 3.2. COMPONENTS OF THE TESTING UNIT

The mechanical parts of the testing unit were made of stainless steel sheet metal and joined together by welding. The wall thicknesses of the condenser section are 5 mm for the covers and 3 mm for fixed parts. In order to prevent the leakage, silicone gaskets have been used under the covers. The whole mechanical system including the process and cooling fans was insulated to reduce thermal losses. The properties of the thermal insulation material are given in Table A.1. The general view of the condenser testing unit is shown in Figure 3.4.



Figure 3.4. Condenser testing unit

As mentioned in the previous chapter, temperature and humidity probes shown in Figure 3.5 have been placed at the inlet and outlet of the condenser section for process cycle and only at the inlet of the condenser section for cooling cycle. The technical specification of the probes is given in Table A.2.



Figure 3.5. Temperature and humidity probes

Calibrated annubars which average the pressure differentials between static and stagnation pressures across the flow section were used to measure volumetric flow rates. As it can be seen from Figure 3.6, the differential pressures from the annubars were measured by the differential pressure sensors, and the flow rates obtained by the sensors were used to control the fan motors via the PLC units. The data sheets of the differential pressure sensors can be found in Table A.3.

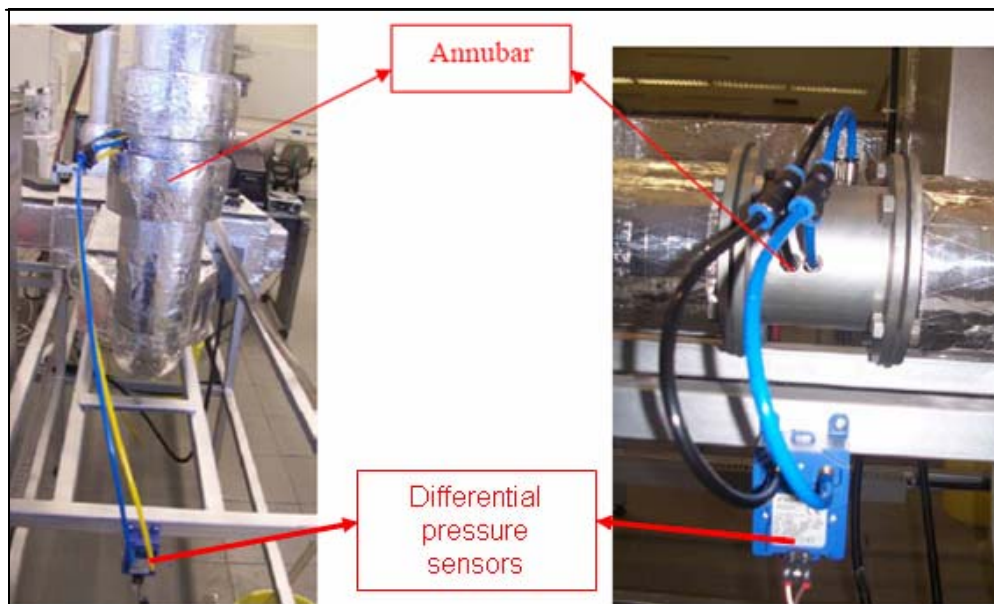


Figure 3.6. Annubars and differential pressure sensors

In order to heat the process air, a 3 kW heater was employed as shown in Figure 3.7. The heater has the resolution of 150W and it is proportionally controlled by the PLC according to the set temperature value.



Figure 3.7. Heater

A humidifier unit shown in Figure 3.8 was located downstream the heater to simulate the vaporization of the water from the laundry in the tumble. A 4kW heater inside the 40-liter water tank of the humidifier evaporates the water, and the vapor flows to a three-way valve. The proportionally controlled valve diverts an amount of vapor that is needed for process air to reach its set relative humidity value into the process channel. The rest is removed from the system.



Figure 3.8. Humidifier Unit

### 3.3. CONTROLLING UNIT AND TESTING PROCEDURE

#### 3.3.1. Controlling Unit

The flow rates, temperature and the humidity of the condenser testing unit are brought to the set conditions by a programmable logic controller (PLC) based proportional integral derivative (PID) system. The PLC unit shown in Figure 3.9 controls the fans, the heater and the valve of the humidifier. PID controller attempts to correct the error between the measured process variables and desired set points by calculating the three separate parameters; the proportion, the integral and derivative values. The proportional value determines the reaction to the current error, the integral value determines the reaction based on the sum of recent errors, and the derivative value determines the reaction based on the rate at which the error has been changing.



Figure 3.9. Control unit

For monitoring the working conditions of the system components and controlling the process, a supervisory control and data acquisition (SCADA) program is used in cooperation with a human machine interface (HMI). The interface brings the ability to change the set points, displays the actual working conditions and also records the data taken from the sensors.

### 3.3.2. Testing Procedure

After installing the condenser that is to be tested to the condenser section and installing, if needed, the process and/or cooling air guiding plates to the inlet guiding areas, the covers of the unit are screwed down and the testing procedure is initiated in the following steps:

- The SCADA program that controls the PID system is activated.
- On the HMI that can be seen on Figure 3.10, the following steps are carried out in order.
  - The humidifier is set to “START” and the tank is filled by turning on the water intake valve. When the tank is full, the water intake valve is turned off.
  - Process and cooling air flow rates are set to the test conditions.

- Process air condenser inlet temperature is set to the test condition.
- Process air condenser inlet relative humidity value is set to the test condition
- The condenser testing unit is activated by setting the main control to “START”.

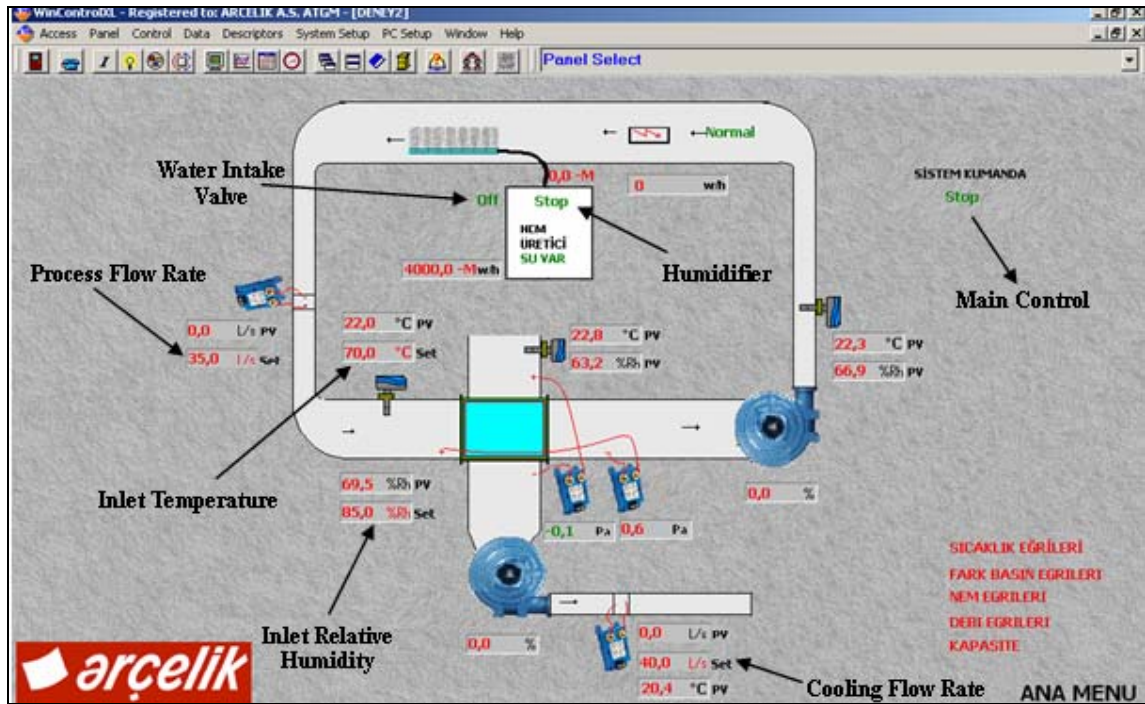


Figure 3.10. Human machine interface (HMI) of the testing unit

- While the testing unit tries to reach the set values, the system is kept under control by checking the temperature and relative humidity change of the system from the graphs that can be drawn by the SCADA program. After initiating the process, as shown in Figure 3.11, the temperature of the process air immediately starts to increase. Since it takes time for the heater within the humidifier tank to heat 40 lt. of water to the boiling temperature, the humidifying process develops slower than the heating process.

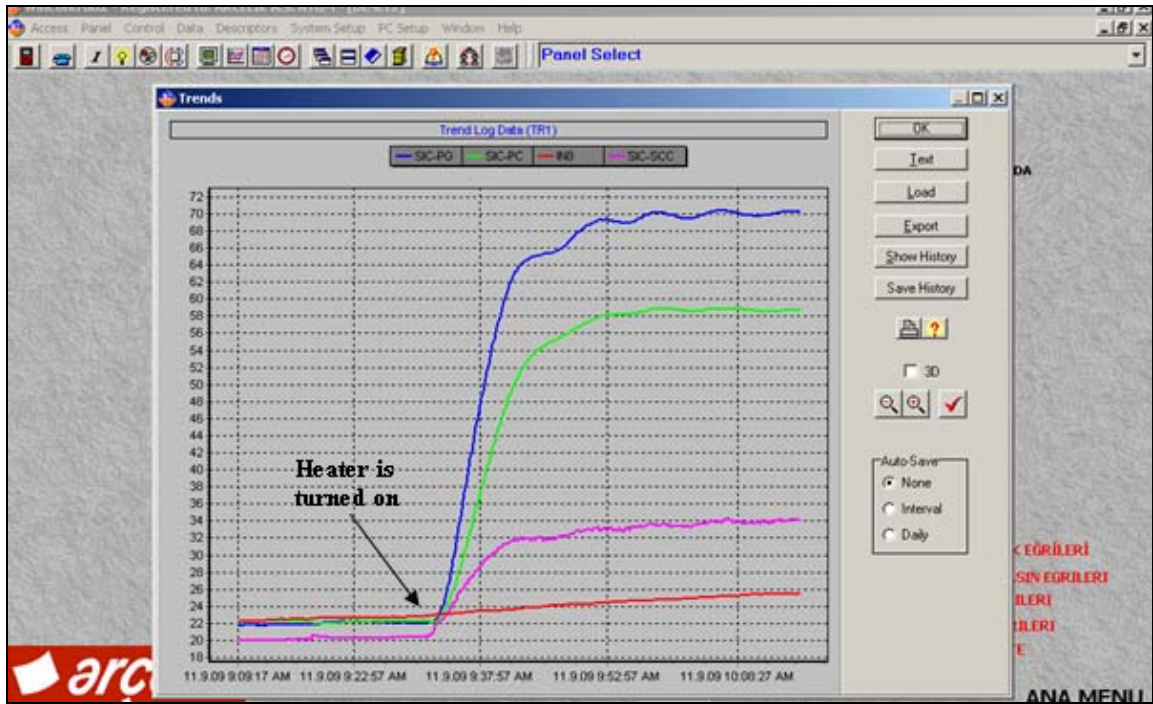


Figure 3.11. The increase of process air temperature

- Before the outlet conditions of the condenser are measured under the steady state condition, the actual values of the system (shown in Figure 3.12) should be matched with the set values. For a steady state to be achieved, the temperature is allowed to oscillate within the range of set value  $\pm 0.3^{\circ}\text{C}$  while the relative humidity and the flow rates are allowed to oscillate within the range of  $\pm 1$  RH and 0.5 lt/s with respect to set values.

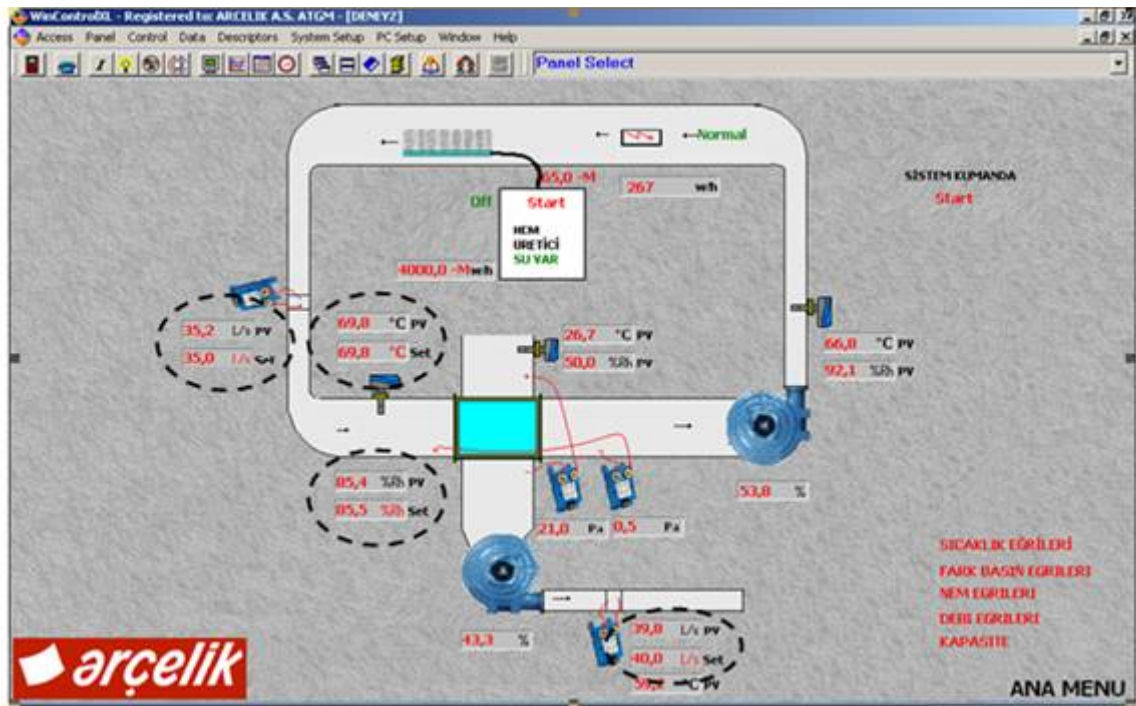


Figure 3.12. Condenser testing unit under steady state conditions

- When the system is balanced with the set condition, condensate is collected in a volumetric container for 5 minutes. At the end of this time period, the collected condensate is weighed as shown in Figure 3.13 and the condensation rate for the given parameters is determined.

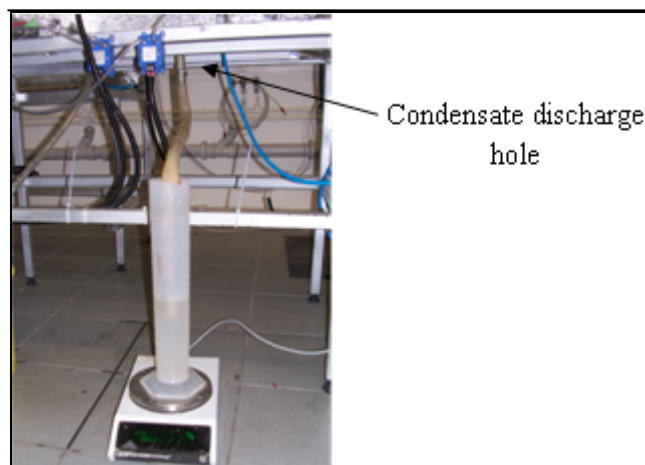


Figure 3.13 Measuring condensation rate



- After the condensation rate is measured, the temperature, relative humidity and flow rate are drawn in graphs as shown in Figure 3.14, 3.15 and 3.16. Finally, all the data that have been recorded with 10s interval are exported to an Excel file for further analysis.

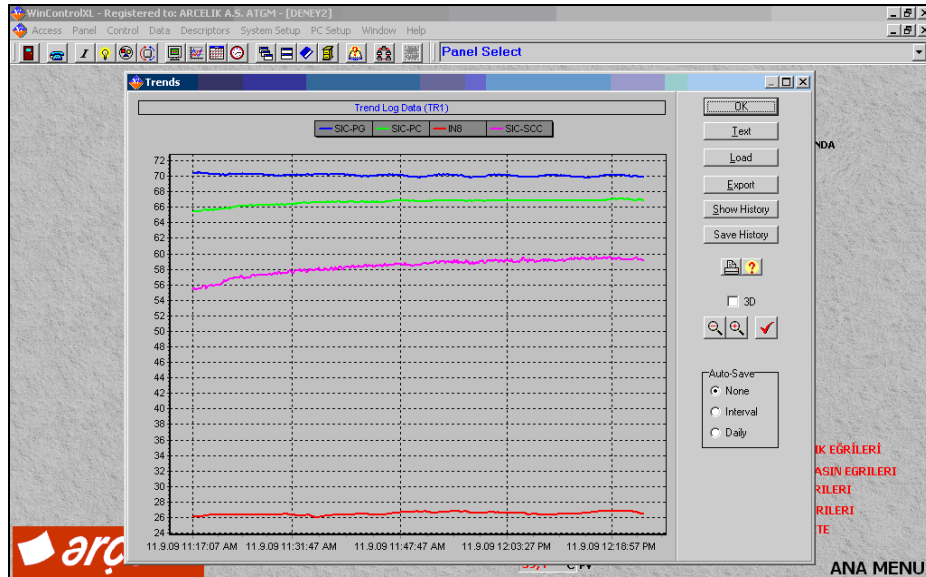


Figure 3.14. Temperature graph

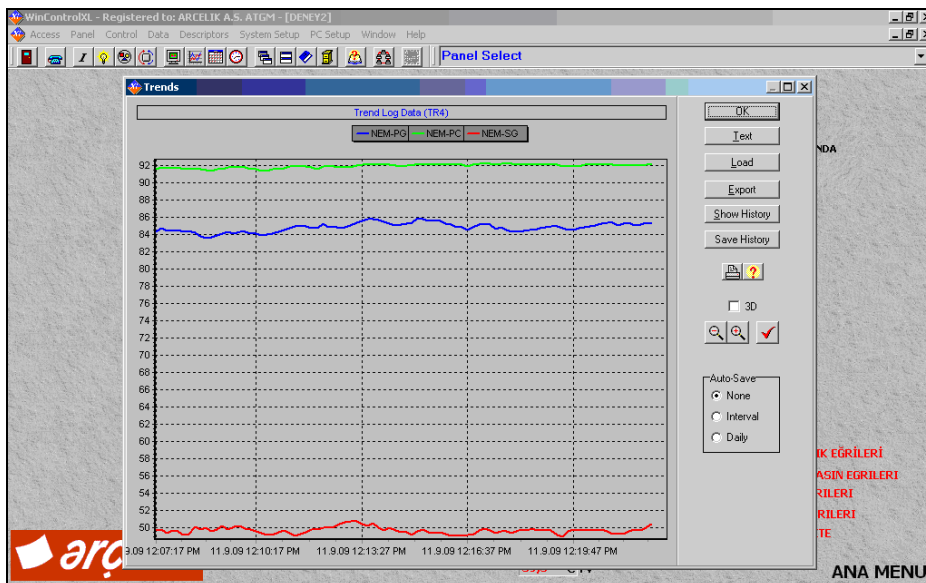


Figure 3.15. Relative humidity graph

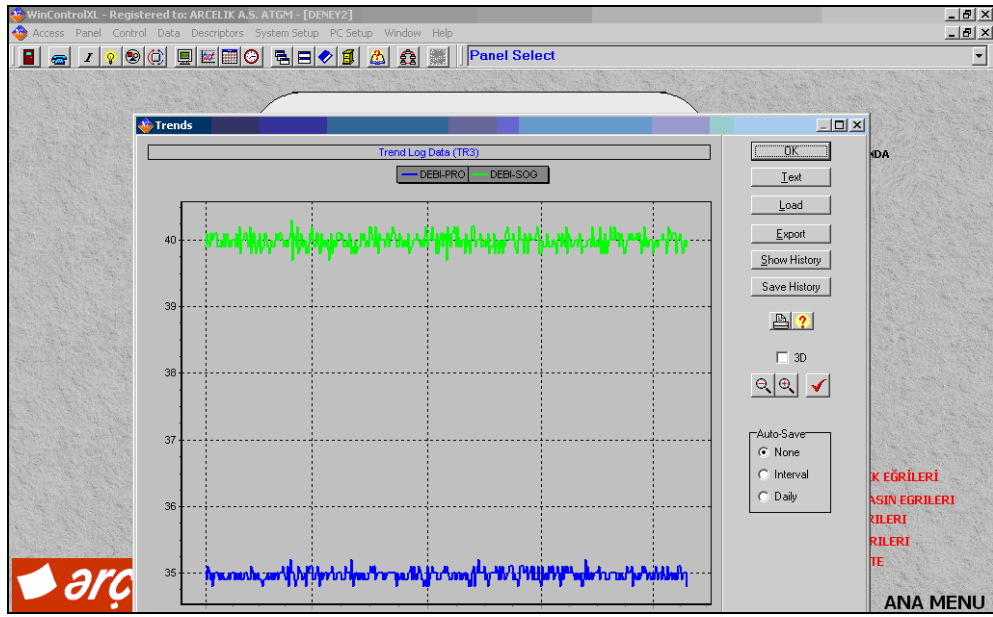


Figure 3.16. Volumetric flow rate graph.

## 4. EXPERIMENTS

### 4.1. DESIGN OF EXPERIMENT

After the completion of the assembly process and calibrating the sensors, a design of experiment (DOE) was formed to measure the performance of the present and newly designed condensers.

DOE is a structured, organized method that was first developed in the 1920s by Sir Ronald A. Fisher, the renowned mathematician and geneticist. It is used to determine the relationship between the different factors affecting a process and the output of that process. A DOE involves designing a set of experiments, in which all relevant factors are varied systematically. When the results of these experiments are analyzed, they help to identify optimal conditions, the factors that influence the results and those that do not, as well as other details such as the existence of interactions.

#### 4.1.1. Data Analysis

The formation of a DOE starts with determining the outputs. In the present study, the condensation rate ( $\dot{m}_{water}$ ) at a steady state condition was selected as the first output, and the condenser efficiency ( $\eta$ ) was chosen as the second output. The condenser efficiency in the testing unit is defined differently from Eq. 2.7 and is calculated by dividing the latent heat taken from the process air per second ( $\dot{E}_{cond}$ ) by the heat transferred to the cooling air per second ( $\dot{E}_{cool}$ ).

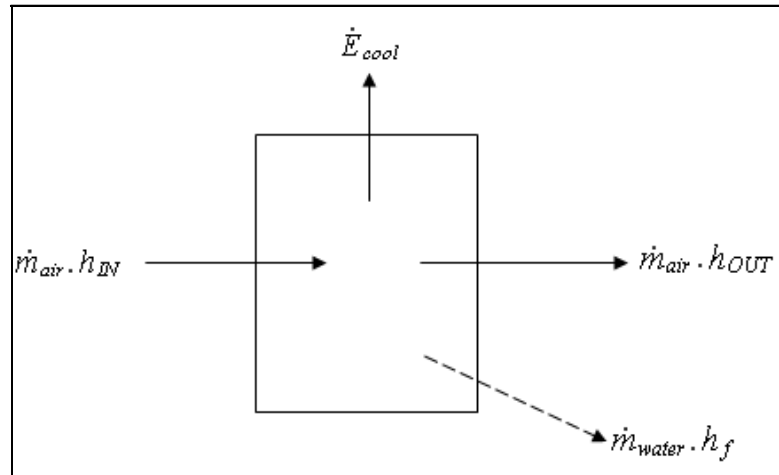


Figure 4.1. Control volume for condenser process channels

Mass conservation for vapor in process air;

$$\dot{m}_{water} = \dot{m}_{air} (w_{IN} - w_{OUT}) \quad (4.1.)$$

Energy conservation for process air,

$$\begin{aligned} \dot{E}_{cool} &= \dot{m}_{air} h_{IN} - \dot{m}_{air} h_{OUT} - \dot{m}_{water} h_f \\ &= \dot{m}_{air} \left( (C_{p_{air}} T_{IN} + w_{IN} h_{gIN}) - (C_{p_{air}} T_{OUT} + w_{OUT} h_{gOUT}) - (w_{IN} - w_{OUT}) h_f \right) \end{aligned} \quad (4.2.)$$

Energy transferred to the cooling air,

$$\dot{E}_{cool} = \dot{m}_{coolingair} \cdot C_{p_{air}} \cdot (T_{C_{OUT}} - T_{C_{IN}}) \quad (4.3.)$$

Energy of condensation,

$$\dot{E}_{cond} = \dot{m}_{water} \cdot h_{fg} = \dot{m}_{air} (w_{IN} - w_{OUT}) \cdot h_{fg} \quad (4.4.)$$

According to the equations shown above, the condenser efficiency is calculated as follows;

$$\eta = \frac{\dot{E}_{cond}}{\dot{E}_{cool}} \quad (4.5.)$$

$$= \frac{(w_{IN} - w_{OUT}) \cdot h_{fg}}{(C_{p_{air}} T_{IN} + w_{IN} h_{gIN}) - (C_{p_{air}} T_{OUT} + w_{OUT} h_{gOUT}) - (w_{IN} - w_{OUT}) h_f}$$

#### 4.1.2. Design of Experiment Parameters

In order to investigate the condensation rate and the condenser efficiency of a condenser, the parameters of the testing unit were chosen as the factors of the DOE as shown in Table 4.1.

Table 4.1 Factors of the DOE

Factors	
Process air flow rate (lt/s)	Qp
Cooling air flow rate (lt/s)	Qc
Process air temperature at condenser inlet (°C)	Tp
Process air relative humidity at condenser inlet %	RHp
Process air inlet channel geometry	Channelp
Cooling air inlet channel geometry	Channelc

After defining the factors and the outputs, a DOE is formed by using Minitab which is a statistical software package that was developed by several researchers at the Pennsylvania State University (Barbara F. Ryan, Thomas A. Ryan, Jr., and Brian L. Joiner) in 1972. MINITAB is often used in conjunction with the implementation of Six Sigma and

it offers four types of designed experiments: factorial, response surface, mixture, and Taguchi (robust).

Among the four types of experiment designs mentioned above, factorial design is the one that allows the simultaneous study of the effects that several factors may have on a process. Without the use of factorial experiments, important interactions may remain undetected. Therefore, a factorial DOE was chosen in the present project.

In order to minimize the time spent for the present experiments, a fractional factorial design was preferred instead of using a full factorial design. The main difference between the full and fractional factorial design is that a full factorial design includes measurements at all combinations of the experimental factor levels while a factorial design consists of a carefully chosen subset (fraction) of the experimental runs of a full factorial design.

As it can be seen from Table 4.2, the quantitative factors that were defined for testing the condensers have two levels. For the purpose of determining these levels, a benchmark study has been made on the working conditions of present air condenser dryers. The measured minimum and maximum values for the process and cooling air flow rates, process air temperature and relative humidity values at the inlet of the condenser were chosen as the levels of the factors. In addition to these quantitative factors, the channel geometries for cooling and process air were also categorized with two levels: straight channel and a channel with 90° curve.

Table 4.2. Factor levels of the DOE

<b>Factors</b>	<b>Min</b>	<b>Max</b>
Process air flow rate (lt/s)	30	55
Cooling air flow rate (lt/s)	30	70
Process air temperature at condenser inlet (°C)	65	75
Process air relative humidity at condenser inlet %	85	95
Process air inlet channel geometry	Straight	Curved
Cooling air inlet channel geometry	Straight	Curved

If a two-level full factorial design of experiment has been chosen for the six factors mentioned above, the DOE would require 64 test runs ( $2^6$ ). Instead of executing such a large test program, a design of  $1/4$  fraction has been chosen to obtain information about main effects and low-order interactions. Moreover, four center points were added to the test runs in order to examine how the condensation rate and condenser efficiencies change between the max and min levels of the quantitative factors,. Consequently a DOE with 20 test runs has been formed as shown in Table 4.3.

Table 4.3. DOE with 20 test runs

<b>Channelp</b>	<b>Channelc</b>	<b>Qp lt/s</b>	<b>Qc lt/s</b>	<b>Tp °C</b>	<b>RHp %</b>
Curved	Curved	30	30	65	95
Curved	Curved	30	70	65	85
Curved	Curved	42,5	50	70	90
Curved	Curved	55	30	75	85
Curved	Curved	55	70	75	95
Curved	Straight	30	30	75	85
Curved	Straight	30	70	75	95
Curved	Straight	42,5	50	70	90
Curved	Straight	55	30	65	95
Curved	Straight	55	70	65	85
Straight	Curved	30	30	75	95
Straight	Curved	30	70	75	85
Straight	Curved	42,5	50	70	90
Straight	Curved	55	30	65	85
Straight	Curved	55	70	65	95
Straight	Straight	30	30	65	85
Straight	Straight	30	70	65	95
Straight	Straight	42,5	50	70	90
Straight	Straight	55	30	75	95
Straight	Straight	55	70	75	85

## 4.2. EXISTING CONDENSER

### 4.2.1. Properties

The existing condenser used in the benchmark tumble dryer was a compact cross flow plate-fin heat exchanger. Plate fin heat exchangers are a type of extended surface heat



exchangers and they are primarily used for gas-to-gas applications like air condenser tumble dryers. It is usually difficult to obtain a desired heat exchange rate between two gases in a limited space available. This is the motivation behind using a “compact” heat exchanger in a dryer. The existing heat exchanger (condenser) had five process air and six cooling air passes as shown in Figure 4.2.

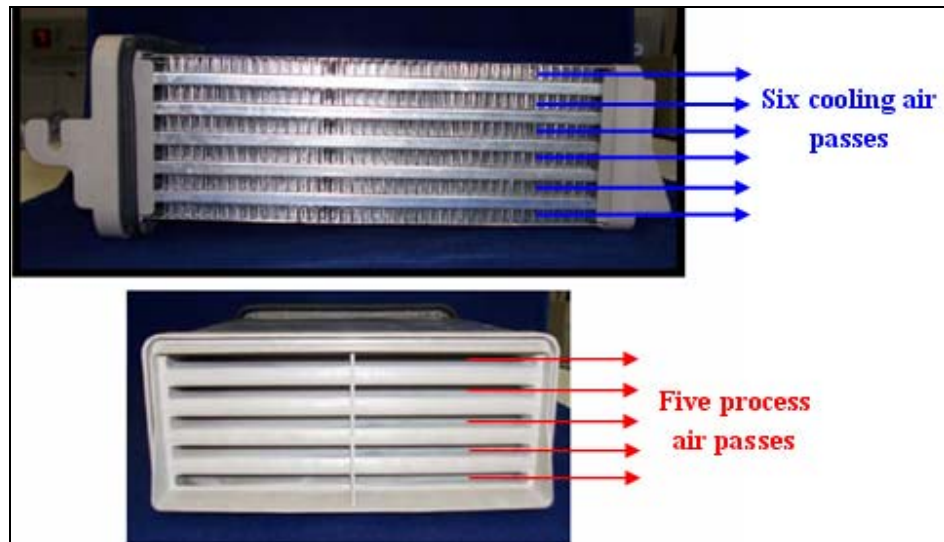


Figure 4.2. The existing condenser

Compact plate fin heat exchangers are widely used in industry especially as a gas-to-gas heat exchanger where condensation or evaporation takes place. With the help of the condensation that occurs within the process air, high heat transfer coefficient values could be obtained. Therefore, the process passes of the condensers contain no fins. The dimension of the process passes that are formed in rectangular shape from aluminum sheet metal with 0.4mm material thickness can be seen on Table 4.4.

Table 4.4. Dimensions of process passes

Number of process passes $N_p$	5
Height of a process pass. $H_p$ (mm)	6,4
Width of a process pass $W_p$ (mm)	182
Length of a process pass $L_p$ (mm)	273

The cooling air passes of the heat exchanger condenser are formed by sandwiching the fins between the process air ducts. The current condenser has six cooling air passes, and the fins within these passes are adhesively bonded to the upper and lower plates of the process passes. The dimensions of the cooling passes can be seen on Table 4.5.

Table 4.5. Dimensions of cooling passes

Number of cooling passes $N_c$	6
Height of a cooling pass. $H_c$ (mm)	7,85
Width of a cooling pass $W_c$ (mm)	234
Length of a cooling pass $L_c$ (mm)	184

The addition of fins to the cooling passes of the condenser increases the heat transfer area and enhances the removal of the condensation heat from the process air. In addition to their thermal benefits, the fins also give structural support to the process passes that are flat rectangular tubes. Figure 4.3 shows many different forms of fins used in the plate fin heat exchangers.

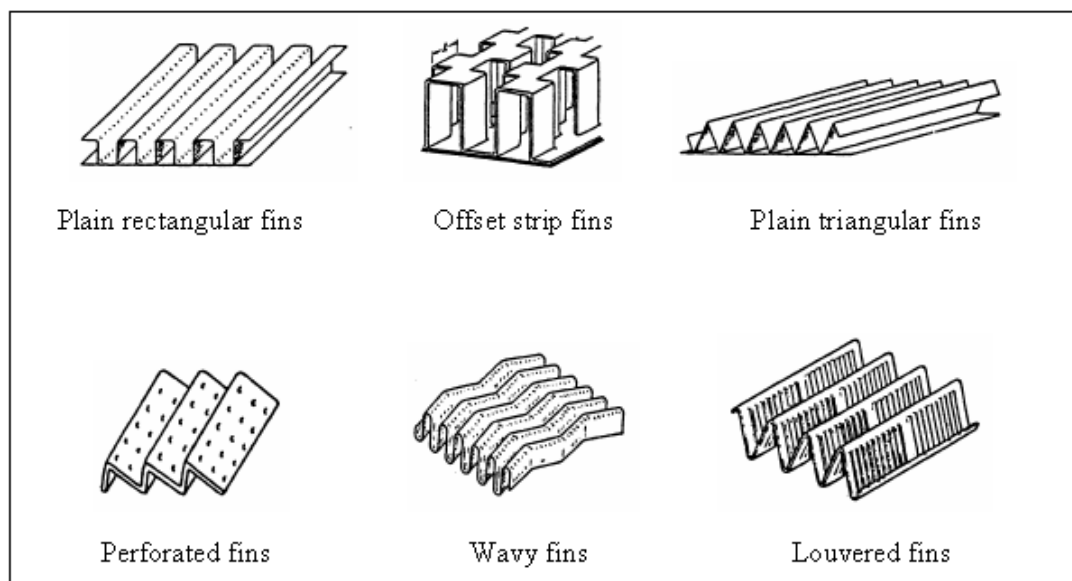


Figure 4.3. Different fin geometries

The fins in the above are designed in such a way to alter gas flow directions, resulting in higher heat transfer. The type of offset strip fins among the different types of fin geometries shown in Figure 4.4 was chosen for the existing condenser.

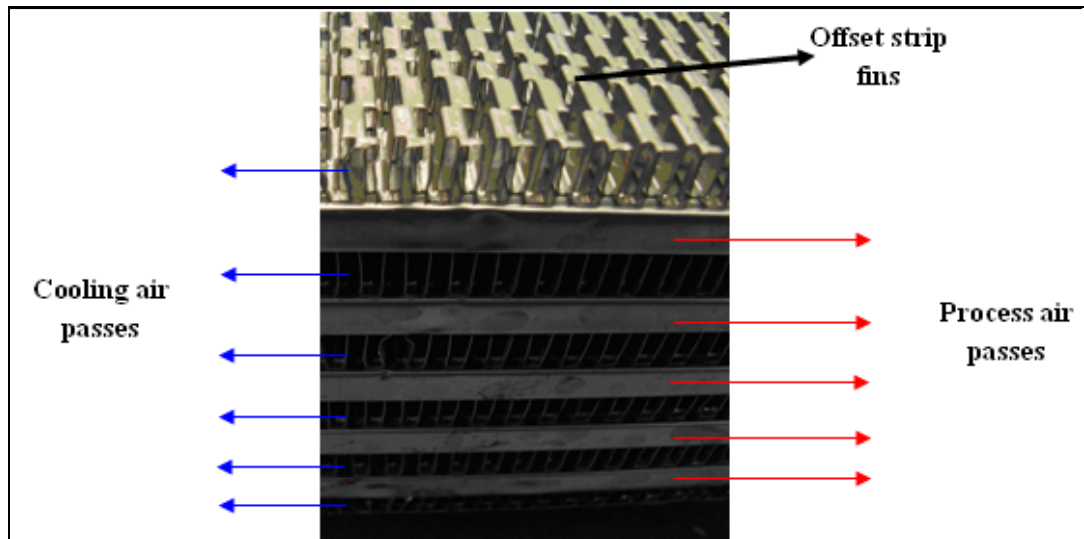


Figure 4.4. Strip fin geometry of existing condenser

As it can be seen from Figure 4.3, the height ( $H$ ) and the width ( $W_{f1}, W_{f2}$ ) of the offset fins are all the same along the cooling pass but there are four different fin lengths ( $L_f$ ) following each other. The dimensions of the offset fin of the existing condenser can be seen on Figure 4.5 below.

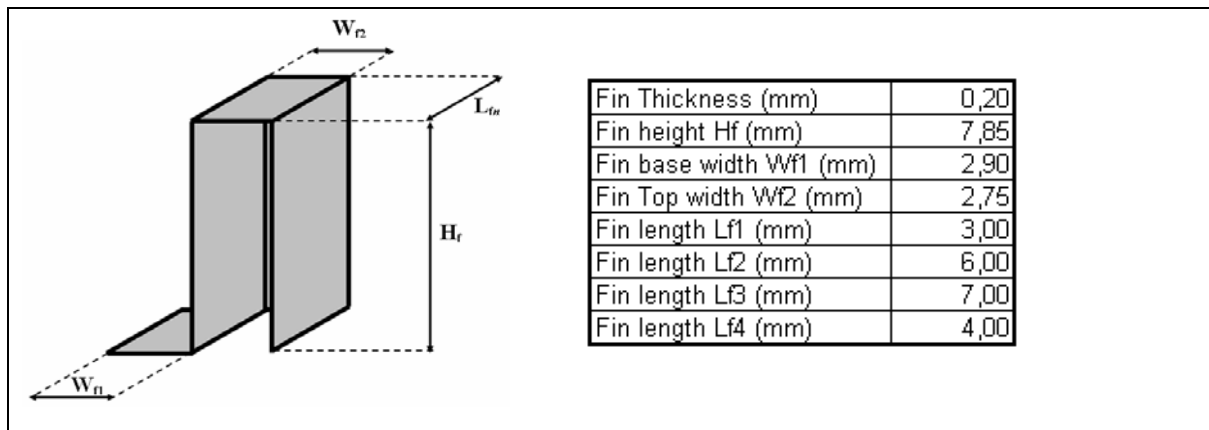


Figure 4.5. Fin dimensions of the existing condenser

#### 4.2.2. Condensation Rate Test Results

After setting up the condenser testing unit and forming a DOE by Minitab, the testing procedure for the present condenser that are used for the Arcelik air condenser dryers was started. The experiments were conducted with 20 different conditions as mentioned on Table 4.3, and as it can be seen on Table 4.6. two tests for each condition was run.

Table 4.6. The condensation rate results

Channelp	Channelc	Qp lt/s	Qc lt/s	Tp °C	RHp %	Condensation Rate gr/s	
						Test 1	Test 2
Curved	Curved	30	30	65	95	0,37	0,32
Curved	Curved	30	70	65	85	0,56	0,54
Curved	Curved	42,5	50	70	90	0,59	0,57
Curved	Curved	55	30	75	85	0,40	0,37
Curved	Curved	55	70	75	95	0,87	0,88
Curved	Straight	30	30	75	85	0,40	0,44
Curved	Straight	30	70	75	95	0,85	0,86
Curved	Straight	42,5	50	70	90	0,52	0,55
Curved	Straight	55	30	65	95	0,28	0,32
Curved	Straight	55	70	65	85	0,60	0,60
Straight	Curved	30	30	75	95	0,47	0,48
Straight	Curved	30	70	75	85	0,88	0,90
Straight	Curved	42,5	50	70	90	0,63	0,64
Straight	Curved	55	30	65	85	0,27	0,30
Straight	Curved	55	70	65	95	0,76	0,69
Straight	Straight	30	30	65	85	0,32	0,34
Straight	Straight	30	70	65	95	0,64	0,62
Straight	Straight	42,5	50	70	90	0,59	0,66
Straight	Straight	55	30	75	95	0,54	0,50
Straight	Straight	55	70	75	85	0,96	0,95

The condensation rates received from the condenser testing unit were entered to the Minitab to analyze the results in a general linear model (GLM). GLM is a statistical tool used by Minitab to analyze and quantify the relationship between the several independent factors and the output. The result of the analysis on the Minitab program can be seen on Figure 4.6. below.

General Linear Model: Cond.Rate versus Channelp; Qp; Qc; Tp; RHp						
Factor	Type	Levels	Values			
Channelp	fixed	2	Curved; Straight			
Qp	fixed	2	30; 55			
Qc	fixed	2	30; 70			
Tp	fixed	2	65; 75			
RHp	fixed	2	85; 95			
Analysis of Variance for Cond.Rate, using Adjusted SS for Tests						
Source	DF	SeqSS	AdjSS	AdjMS	F	P
Channelp	1	0,02880	0,02880	0,02880	41,89	0,000
Qp	1	0,00281	0,00281	0,00281	4,09	0,055
Qc	1	1,14005	1,14005	1,14005	1658,25	0,000
Tp	1	0,32401	0,32401	0,32401	471,29	0,000
RHp	1	0,01201	0,01201	0,01201	17,47	0,000
Channelp*Qp	1	0,00361	0,00361	0,00361	5,25	0,032
Qp*Qc	1	0,01201	0,01201	0,01201	17,47	0,000
Qc*Tp	1	0,03511	0,03511	0,03511	51,07	0,000
Tp*RHp	1	0,00320	0,00320	0,00320	4,65	0,042
Error	22	0,01513	0,01513	0,00069		
Total	31	1,57675				
S = 0,0262202    R-Sq = 99,04%    R-Sq(adj) = 98,65%						

Figure 4.6. GLM results of the existing condenser

The factors and some of their interactions that affect the condensation rate are shown on the “Source” column in Figure 4.5. Since these terms have the values of P’s smaller than 0.05, the null hypothesis is rejected, meaning that the factors and their interactions listed on the “Source” column take role on determining the output which is the condensation rate in this case. Though the value of P for the process air flow rate (Qc) is bigger than 0.05, however, it is also determined as a factor affecting the condensation rate. It is because its interaction with the cooling air flow rate has a value of P smaller than 0.05. Though not presented here, the GLM analysis shows that the cooling air channel geometry (Channelc) has no effect as the condensation rate.

Another output of the analysis to be considered is the R-square adjusted value shown at the end of Figure 4.5. R-sq(adj) is a mathematical term that states how much of the total variation on the output can be explained by the factors on the “Source” column. According to the GLM analysis, the factors and their interactions are responsible for 98.7 per cent of the change of the condensation rate.

After determining the effective factors and interactions, the effect of each term on the condensation rate was examined individually. As it can be seen from Figure 4.7, it is apparent that the cooling air flow rate has the largest effect on the condensation rate. The condensation rate changes in a range between 0.4 – 0.8 gr/s, depending on the cooling air flow rate while it is less affected by the other factors.

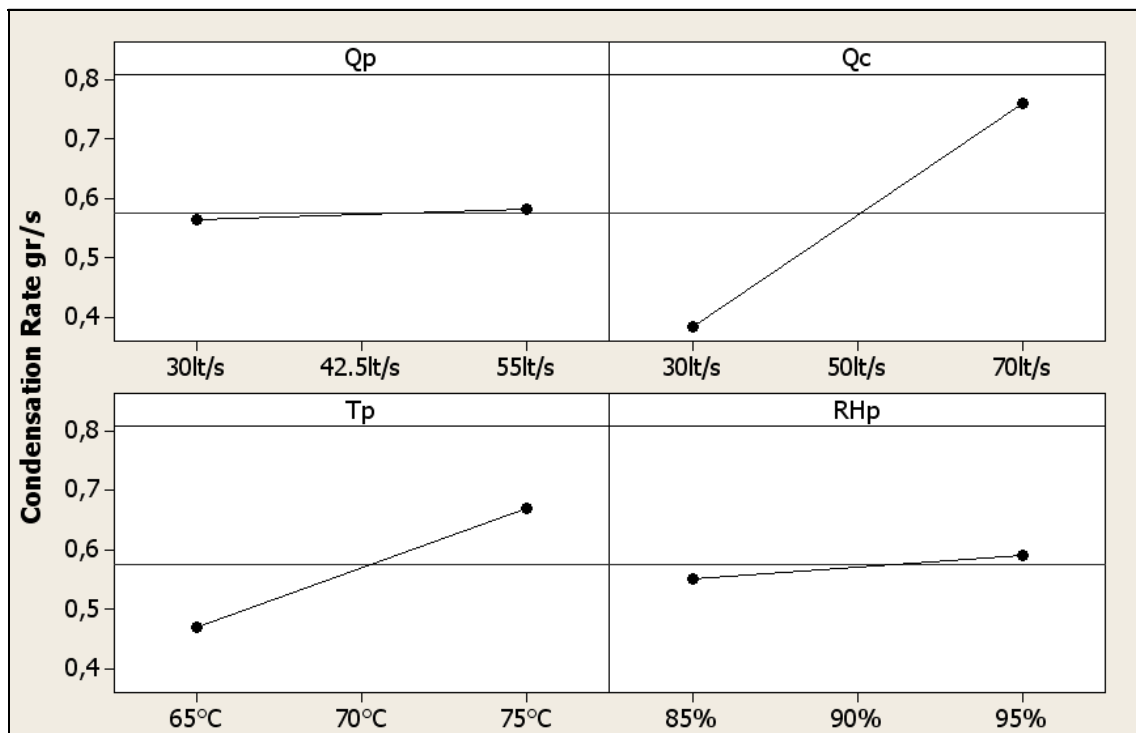


Figure 4.7. Effects of quantitative factors

When the effect of the process channel geometry is examined, as shown in Figure 4.8, it appears that the straight process channel causes higher condensation rates. When the process air flows into the condenser with a 90° curved channel, all the width of the process

passes might not be used properly and as a result the condensation might occur only on a portion of the passes.

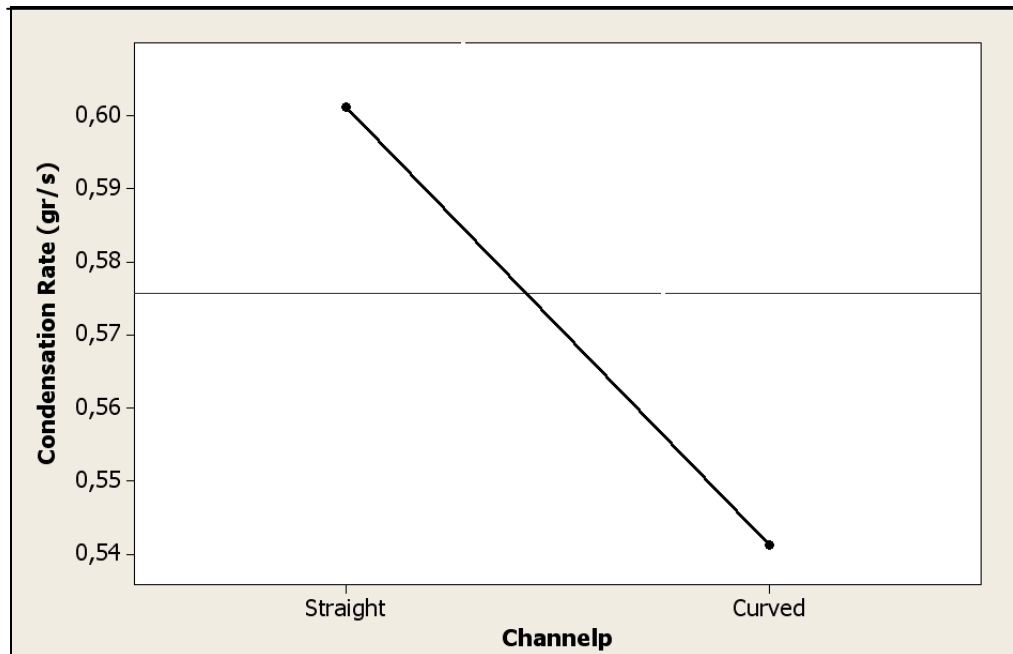


Figure 4.8. Effect of process channel geometry on condensation rate

Total 40 tests on 20 different conditions have been conducted on the present condenser with five process passes, and the mean condensation rate of all tests was determined as 0.58 gr/s.

After examining the effects of the factors individually, the effect ratio of each factor was investigated. In order to determine which the factors should first be focused on, the sum of square value of the factors was examined. The sum of square values of the factors is calculated by Minitab and shown in Figure 4.6 under AdjSS column. The sum of square values represents a measure of variation or derivation from the mean and calculated as a summation of the squares of the differences from the mean. Dividing a sum of square of a factor by the total sum of squares yields the effect ratio of that factor. The effect ratio is an indicative of whether a change of the factor may cause a significantly different output or not.

The effect ratio of each factor is presented in Figure 4.9. It is evident from the figure that the most effective factor on the condensation rate is the cooling air flow rate with the effect ratio of 72.9 per cent.

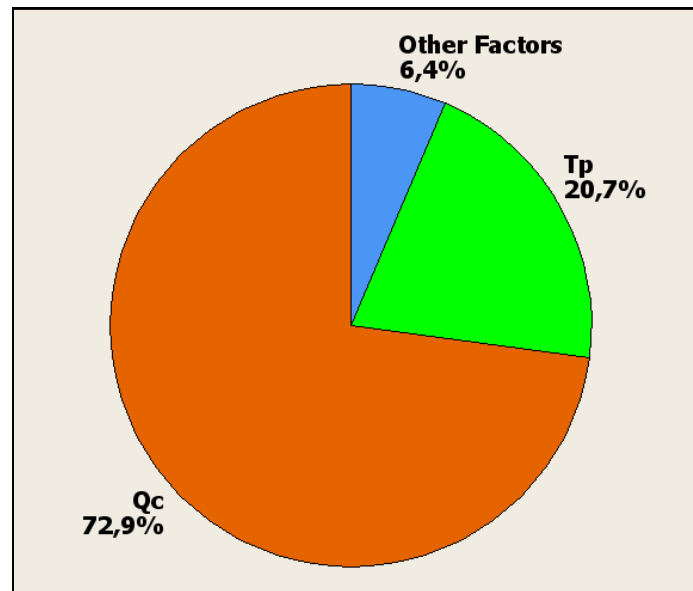


Figure 4.9. Effect ratios of factors on condensation rate

#### 4.2.3. Condenser Efficiency Test Results

After defining the important factors that affect the condensation rate, the same GLM analysis procedure is repeated for condenser efficiency. The condenser efficiency is calculated by Equation 4.3 using the measured condensation rate, cooling air condenser inlet and outlet temperatures and also flow rates, and its values for the 40 test runs are shown in Table 4.7.



Table 4.7. Condenser efficiency results

Channelp	Channelc	Qp lt/s	Qc lt/s	Tp °C	RHp %	Condenser Efficiency $\eta$	
						Test 1	Test 2
Curved	Curved	30	30	65	95	0,76	0,75
Curved	Curved	30	70	65	85	0,69	0,68
Curved	Curved	42,5	50	70	90	0,71	0,74
Curved	Curved	55	30	75	85	0,67	0,68
Curved	Curved	55	70	75	95	0,73	0,72
Curved	Straight	30	30	75	85	0,74	0,76
Curved	Straight	30	70	75	95	0,76	0,75
Curved	Straight	42,5	50	70	90	0,68	0,69
Curved	Straight	55	30	65	95	0,62	0,69
Curved	Straight	55	70	65	85	0,69	0,67
Straight	Curved	30	30	75	95	0,77	0,79
Straight	Curved	30	70	75	85	0,77	0,75
Straight	Curved	42,5	50	70	90	0,73	0,78
Straight	Curved	55	30	65	85	0,62	0,68
Straight	Curved	55	70	65	95	0,73	0,76
Straight	Straight	30	30	65	85	0,71	0,73
Straight	Straight	30	70	65	95	0,72	0,71
Straight	Straight	42,5	50	70	90	0,76	0,73
Straight	Straight	55	30	75	95	0,85	0,79
Straight	Straight	55	70	75	85	0,75	0,75

After entering the measured condenser efficiency values to the Minitab, the GLM analysis was performed and the important factors were determined as shown in Figure 4.10. According to the GLM, similar to the condensation rate, it is found out that the cooling air condenser inlet geometry has no effect on condenser efficiency. The value of R-sq(adj) indicates that the factors and their interactions are responsible for the change of the condensation efficiency with 65.6 per cent.

General Linear Model: Ec versus Channelp; Qp; Qc; Tp; RHp			
Factor	Type	Levels	Values
Channelp	fixed	2	Curved; Straight
Qp	fixed	2	30; 55
Qc	fixed	2	30; 70
Tp	fixed	2	65; 75
RHp	fixed	2	85; 95

Analysis of Variance for Ec, using Adjusted SS for Tests						
Source	DF	SeqSS	AdjSS	Adj MS	F	P
Channelp	1	0,0084500	0,0084500	0,0084500	10,18	0,004
Qp	1	0,0060500	0,0060500	0,0060500	7,29	0,012
Qc	1	0,0000125	0,0000125	0,0000125	0,02	0,903
Tp	1	0,0210125	0,0210125	0,0210125	25,33	0,000
RHp	1	0,0098000	0,0098000	0,0098000	11,81	0,002
Channelp*Qp	1	0,0050000	0,0050000	0,0050000	6,03	0,022
Qp*Qc	1	0,0045125	0,0045125	0,0045125	5,44	0,028
Error	24	0,0199125	0,0199125	0,0008297		
Total	31	0,0747500				

S = 0,0288043    R-Sq = 73,36%    R-Sq(adj) = 65,59%

Figure 4.10. GLM results for condenser efficiency

Next the effect of the quantitative factors on condenser efficiency was examined. As it can be seen from Figure 4.11, the condenser efficiency for the present condenser with five process and six cooling passes varies within a range of 70 – 75 per cent.

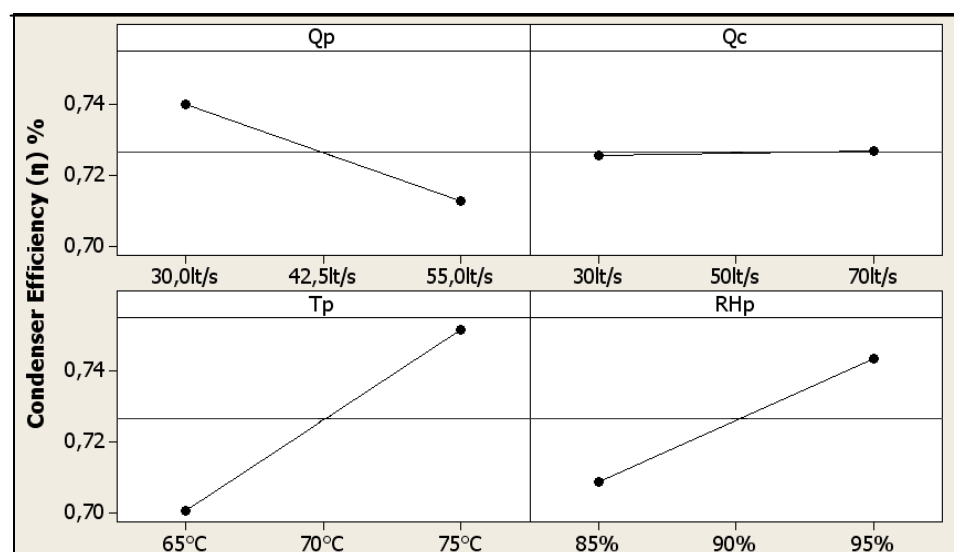


Figure 4.11. Effects of quantitative factors on condenser efficiency

The effect of the process channel geometry on the condensation rate is examined in Figure 4.12. It is apparent that the straight process channel yields higher condensation rates. The mean value of the condenser efficiency for 40 tests was 72.7 per cent.

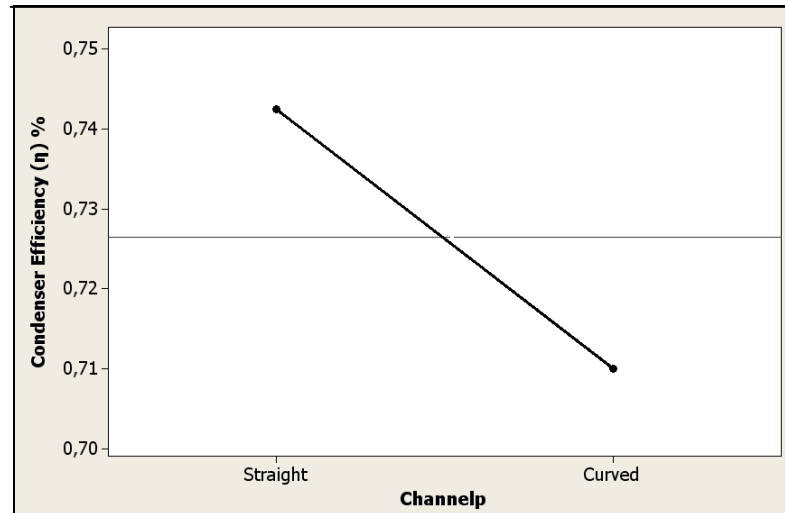


Figure 4.12. Effect of the process channel geometry on the condenser efficiency

The examination of the sum of square values of the factors shows that the most effective factors on condenser efficiency are the process air temperature with 28.1 per cent, the relative humidity of the process air with 13.1 per cent and the condenser inlet channel geometry of the process air with 11.3 per cent.

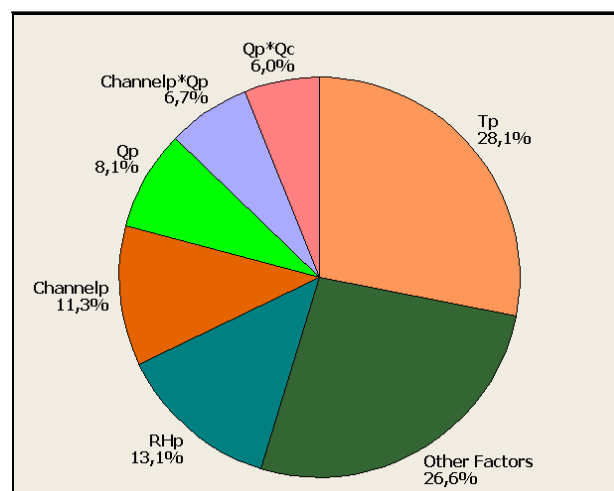


Figure 4.13. Effect ratios of factors on condenser efficiency

## 5. DESIGN OF THE NEW CONDENSER

After finishing the experiments with the existing condenser, started to design a new condenser with higher condensation rate and efficiency. As a first step of the study the constraints have been stated.

### 5.1. CONSTRAINTS

Changing the outer dimensions of the condenser would cause a modification within the plastic injection moulds of the base chassis. Since this operation would take a lot of time and be very costly, for the new condenser it was decided to keep the outer dimension the same with the existing one. The main dimensions of the condenser can be seen on Figure 5.1 below.

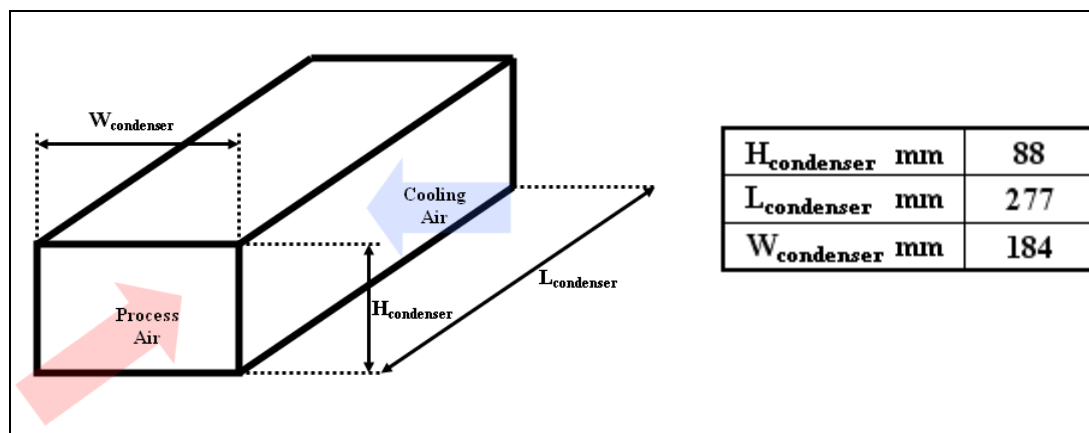


Figure 5.1. Outer dimensions of the condenser

The production of a plate-fin heat exchanger is a very hard process. Bending and clamping the aluminum sheet metal for forming the rectangular process channel tubes and adhesive bonding of the strip fins to the channels require a high precision production line. This was the main motivation behind getting help from the company that produces the existing condenser for the production of the new condenser prototypes. In order to assure the congruity with the production line, for the new condenser the material and the

thickness of the aluminum plates were not changed. The thickness of the tube plates were fixed as 0,4 mm and the thickness of the strip fins were fixed as 0.2 mm.

Another point that was considered for the new condenser was the production costs. In the competitive market of the air condenser dryers, reducing the cost of the condenser comes into question because it is the most costly component of the dryer. Therefore, the condenser that would be developed should decrease the production costs by reducing the material and/or facilitating the production process.

## 5.2. DESIGN OF THE PROCESS PASSES

After determining the constraints, the designing procedure for the process channels was started. For this purpose firstly a literature survey was carried out and the effective parameters for air-vapor mixture film condensation were listed. As it can be seen from Figure 5.2. in the presence of the non-condensable gases it is not possible for the condensate to fill up the whole channel. Due to large difference in density between the gas and the liquid phases, a small amount of air occupies much of the space when condensation occurs. In addition to this, even when the whole domain of the channel is at the same temperature as the bottom wall, a small amount of vapor still remains in the air as moisture.

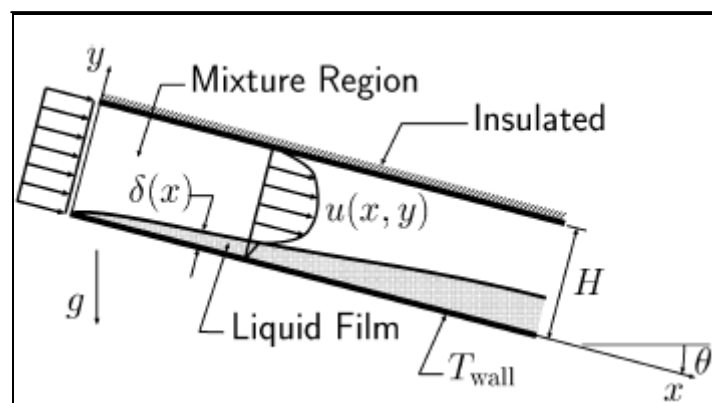


Figure 5.2. Film condensation [11]

In his study Siow developed a numerical solution of a two phase model for laminar film condensation of a vapor-air mixture in channel [11]. For the input parameters listed below, his studies showed that the film thickness of the condensate ( $\delta_{(x)}$ ) does not grow exponentially at the end portion but it stays at a constant level. As it can be seen from Figure 5.3, with the given input parameters, the ratio of the condensate film thickness to the height of the channel ( $\delta^*$ ) is constant for  $x^*$  values higher than 600.  $x^*$  is the ratio of the distance from the inlet of the channel ( $x$ ) to the height ( $H$ ) of the channel

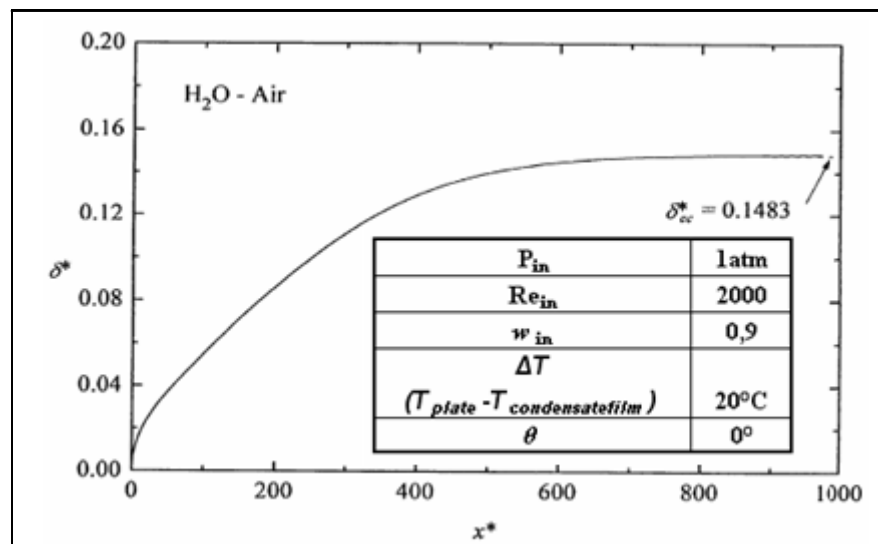


Figure 5.3. The growth of condensate film thickness [11]

In his study Siow also showed that heat transfer is strongly reduced as the film thickness increases early in the condensation process. As shown on Figure 5.4. the heat transfer is continuously reduced because of the reduction of the interface temperature between the condensate film and the mixture region though the film thickness does not change too much. In Figure 5.4. the heat transfer rate was represented by the variation of the local Nusselt number ( $Nu_x$ ).

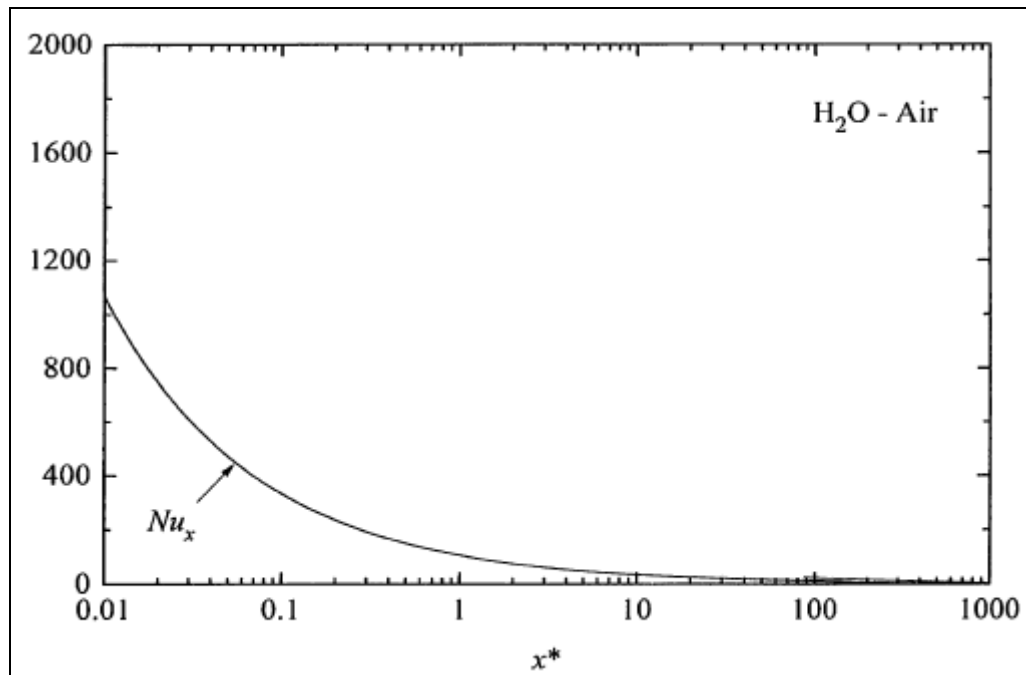


Figure 5.4. The change of local Nusselt number [11]

In their study, Ormiston, Siow and Soliman showed that an increase in angle of declination ( $\theta$ ) results in a thinner and faster moving liquid film and this enhances the heat transfer [12].

According to the studies mentioned above, it was decided to increase the height of the process pass in the new condenser for decreasing the condensate film thickness and increasing the heat transfer. In the new condenser the height of the process channels were increased from 6,4 to 8,5mm. In order to prevent the over narrowing of the cooling passes, the number of the process passes were reduced from six to five. As the height of each process passes was increased, it was expected to reduce the film thickness and pressure losses along the condenser and also enhance the heat transfer rate. Although the positive effect of increasing the declination angle was known, the angle was not changed in order to prevent the necessary modifications on the plastic injection moulds. The process channel dimensions of the new condenser can be seen on Table 5.1.

Table 5.1. Dimensions of the process passes

Number of process passes $N_p$	4
Height of a process pass. $H_p$ (mm)	8,5
Width of a process pass $W_p$ (mm)	181
Length of a process pass $L_p$ (mm)	277

### 5.3. DESIGN OF THE COOLING PASSES

Since the outer dimensions of the condenser were fixed, after specifying the process passes dimensions, the dimensions of the cooling passes were formed automatically. The dimensions of the cooling passes can be seen on Table 5.2.

Table 5.2. Dimensions of the cooling passes

Number of cooling passes $N_c$	5
Height of a cooling pass. $H_c$ (mm)	9,86
Width of a cooling pass $W_c$ (mm)	234
Length of a cooling pass $L_c$ (mm)	184

According to the cooling channel dimensions, a method for comparing the effect of different fin geometries on convective heat transfer coefficient has been defined. In order to make a comparison, the height of the fin geometry was cut from the middle and as can be seen from Figure 5.5, the air flow within the cooling pass was modeled as a forced convection over a flat plate.



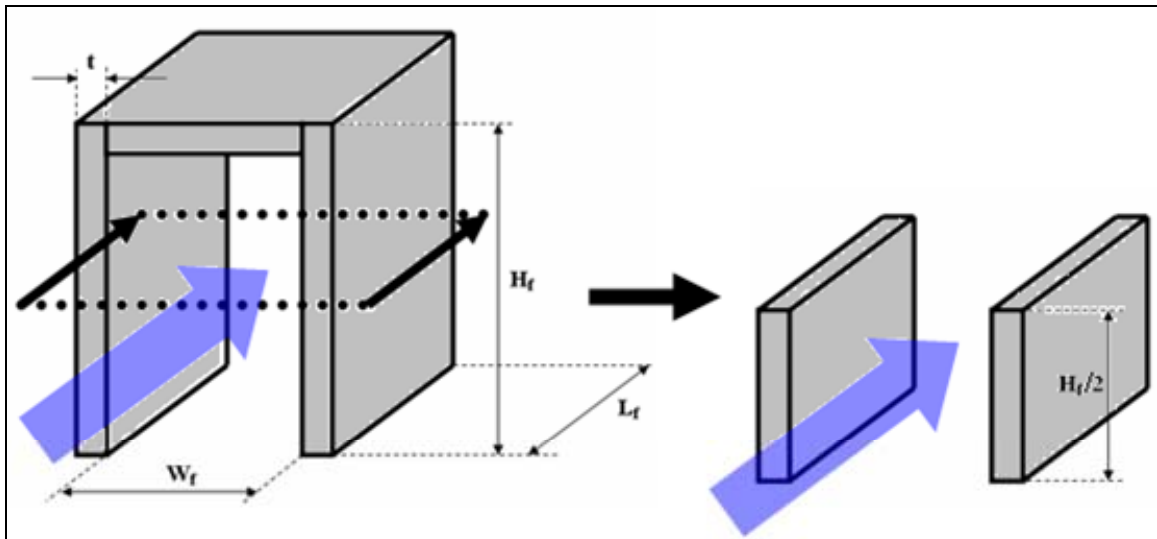


Figure 5.5. Model for fin geometry

For determining the average convection heat transfer coefficient, a steady, incompressible, laminar flow was assumed over the fin with constant fluid properties and negligible viscous dissipation. The cross section area ( $A_{CROSS}$ ) that the cooling air flows was calculated with the formula given below.

$$A_{CROSS} = \left( W_c - \frac{2 \cdot W_c \cdot t}{2 \cdot t + W_{f1} + W_{f2}} \right) \cdot H_c \cdot N_c \quad (5.1)$$

The velocity of the cooling air within the condenser ( $V_C$ ) was calculated by dividing the volumetric flow rate ( $Q_C$ ) to the cross section area.

$$V_C = \frac{Q_C}{A_{CROSS}} \quad (5.2)$$

The Reynolds number for the flow was calculated by using the calculated velocity of cooling air, the length of the fin ( $L_f$ ) and also the kinematic viscosity ( $\nu$ ) of the air. Since the Prandtl number for air was higher than 0.6, the Nusselt number on the fin surface was calculated with the Formula 5.4.

$$Re = \frac{V_c \cdot L_f}{\nu} \quad (5.3.)$$

$$Nu = 0,664 \cdot \sqrt{Re} \cdot \sqrt[3]{Pr} \quad (5.4.)$$

The convection heat transfer coefficient was determined by multiplying the Nusselt number with the thermal conductivity of the air ( $k_f$ ) and dividing by the length of the fin.

$$h = \frac{k_f \cdot Nu}{L_f} \quad (5.5.)$$

After determining the heat transfer coefficient, thermal performances of the fins were compared by their fin efficiencies ( $\eta_f$ ). The fin efficiency is the ratio of the actual heat transferred by a fin to the heat that would be transferred if the entire fin height is at the fin base temperature. The formula for the fin efficiency is:

$$\eta_f = \frac{\tanh(m \cdot L_C)}{m \cdot L_C} \quad (5.6.)$$

In order to calculate the fin efficiency, the calculated convection heat transfer coefficient and the thermal conductivity of the fin ( $k_s$ ) are used as follows:

$$m \cdot L_C = \left( \frac{h \cdot P}{k_s \cdot A_C} \right)^{1/2} \cdot L_C \quad (5.7.)$$

For a straight fin of a rectangular cross section, the perimeter ( $P$ ), the corrected length ( $L_C$ ) and the corrected area ( $A_C$ ) are calculated as follows.

$$P = 2 \cdot (t + L_f) \quad (5.8.)$$

$$L_C = (H_f + t)/2 \quad (5.9.)$$

$$A_C = t.L_f \quad (5.10.)$$

The formed model was used for analyzing the effect of the geometrical parameters on convective heat transfer coefficient and fin efficiency. For all analysis thermal conductivity of the aluminum fin material ( $k_s$ ) and air ( $k_f$ ) were fixed as 200 W/mK and 0.027 w/mK. The Prandtl number of the air was fixed as 0.7 and also the kinematic viscosity of the air was fixed as  $1.7 \cdot 10^{-5} \text{ m}^2/\text{s}$ . In the first part of the analysis the fin height, thickness and length were kept constant and the fin width ( $W_f$ ) was changed. As it can be seen from Figure 5.6, the change of the fin width had a very limited effect on the convective heat transfer coefficient and fin efficiency. Changing the fin width from 0,5 mm to four mm increased the fin efficiency from 95.4 per cent to 95.5 per cent and decreased the convective heat transfer coefficient from 111.3 to 108.4 W/m<sup>2</sup>K.

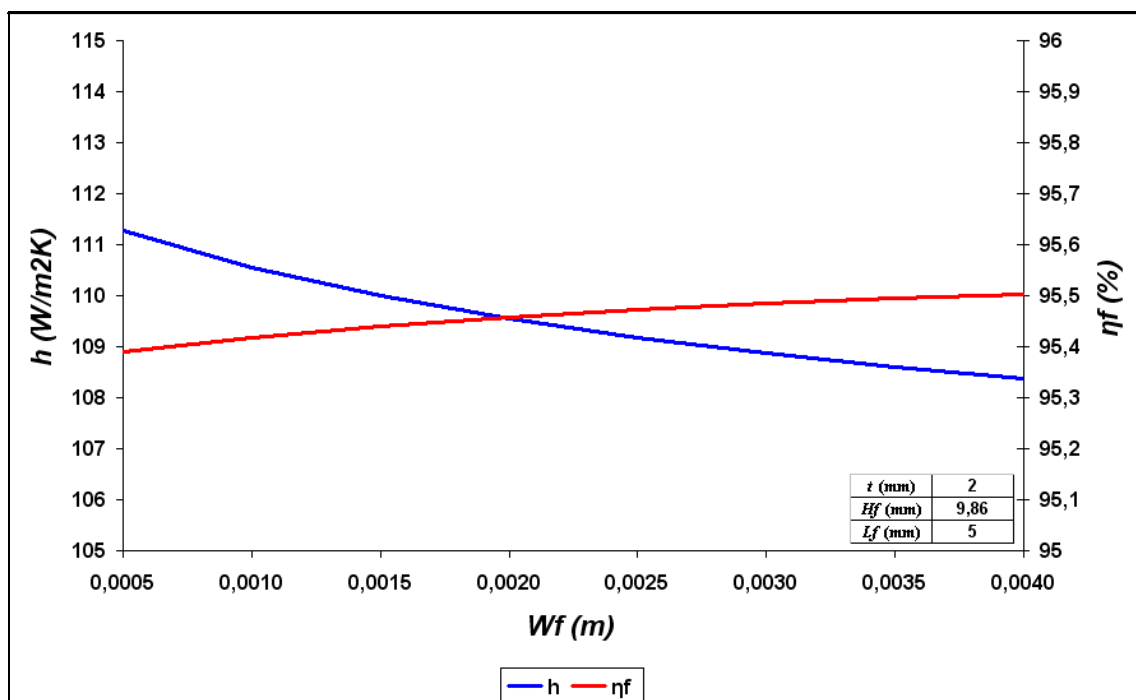


Figure 5.6. Effect of fin width

In the second part of the analysis the fin length was examined. It was understood that when the other dimensions were fixed, increasing the fin length causes an increase in the fin efficiency and a decrease in the convective heat transfer coefficient. As it can be seen

from Figure 5.7, changing the fin length from one to ten mm increased the fin efficiency from 89.2 per cent to 96.8 per cent and decreased the convective heat transfer coefficient from 244 to 77 W/m<sup>2</sup>K.

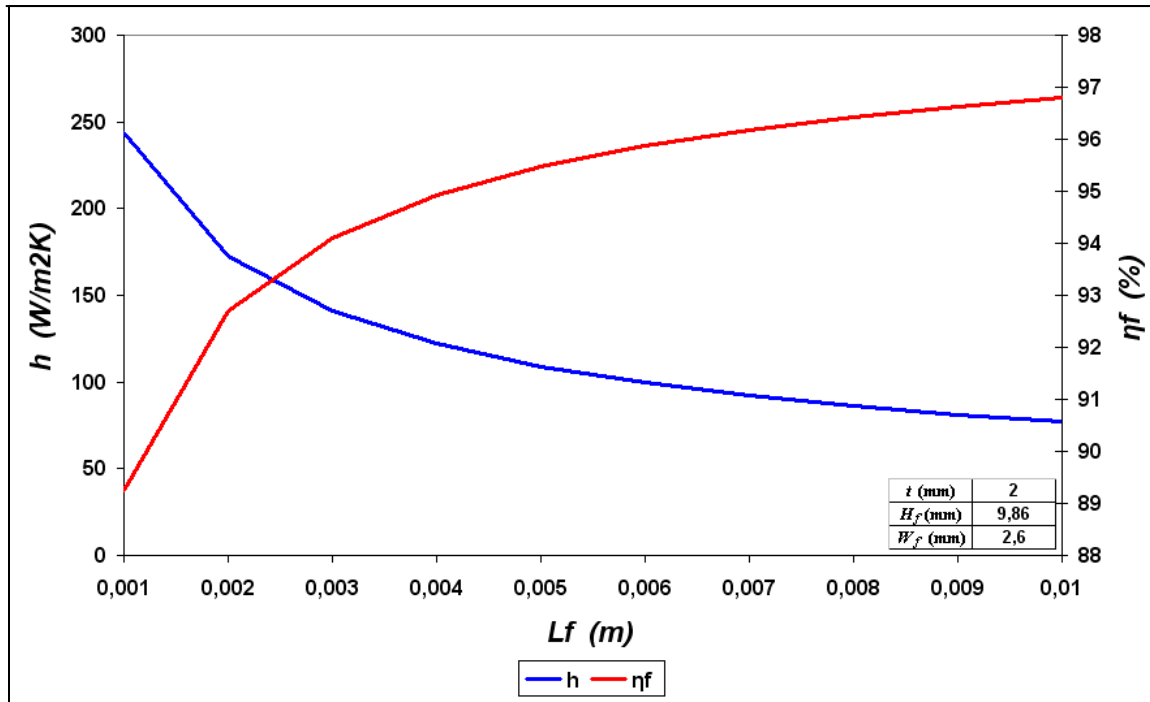


Figure 5.7. Effect of fin length

Considering the mentioned outputs and the production constraints, the fin dimensions of the new condenser that can be on Table 5.3. were determined.

Table 5.3. Fin dimensions of the new condenser

Fin height $H_f$ (mm)	9,86
Fin base width $W_{f1}$ (mm)	3
Fin Top width $W_{f2}$ (mm)	2,6
Fin length $L_{f1}$ (mm)	3
Fin length $L_{f2}$ (mm)	4
Fin length $L_{f3}$ (mm)	6
Fin length $L_{f4}$ (mm)	7

As it can be seen from Figure 5.8, increasing the fin height effects both convective heat transfer coefficient and fin efficiency in a negative way. Since the height of the fin was increased from 7.85 to 9.86 mm in the new condenser, by choosing the fin dimensions mentioned above it was aimed to minimize this negative effect. The calculated convective heat transfer coefficient and the fin efficiency of the existing condenser was 111.7 W/m<sup>2</sup>K and 97 per cent. Thanks to the new fin dimensions, the convective heat transfer coefficient and the fin efficiency could be calculated as 109.1 W/m<sup>2</sup>K and 95.5 per cent.

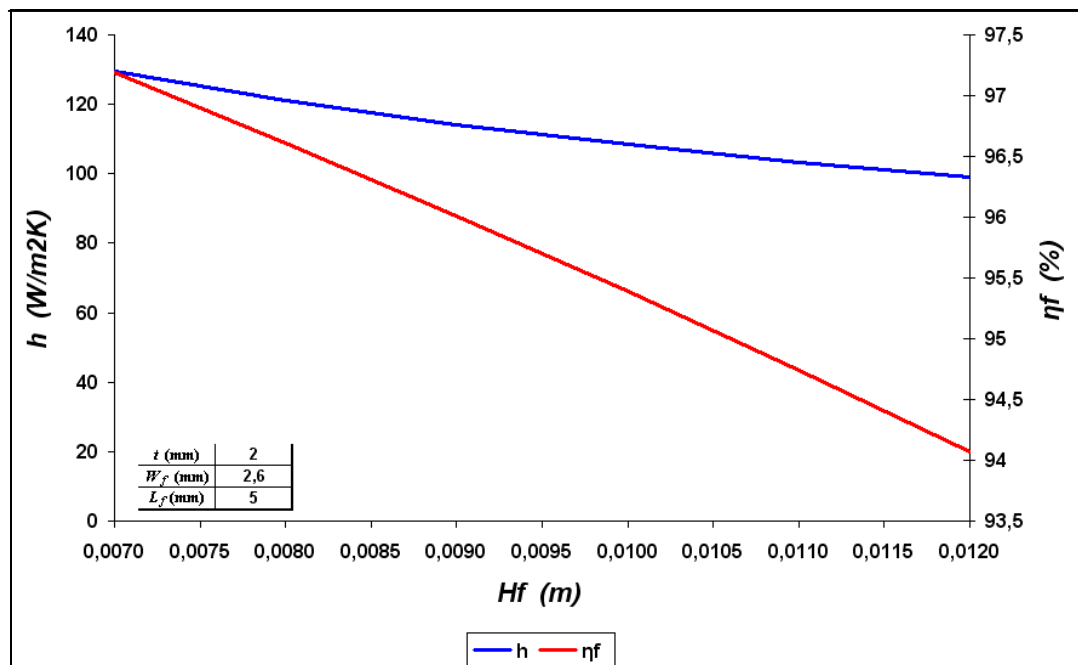


Figure 5.8. Effect of fin height

#### 5.4. TEST RESULTS

The prototype condenser with the dimensions described in the previous section was installed to the condenser section of the condenser testing unit as shown in Figure 5.9. The tests were conducted with the same parameters as those used in the DOE for the original five process pass benchmark condenser.

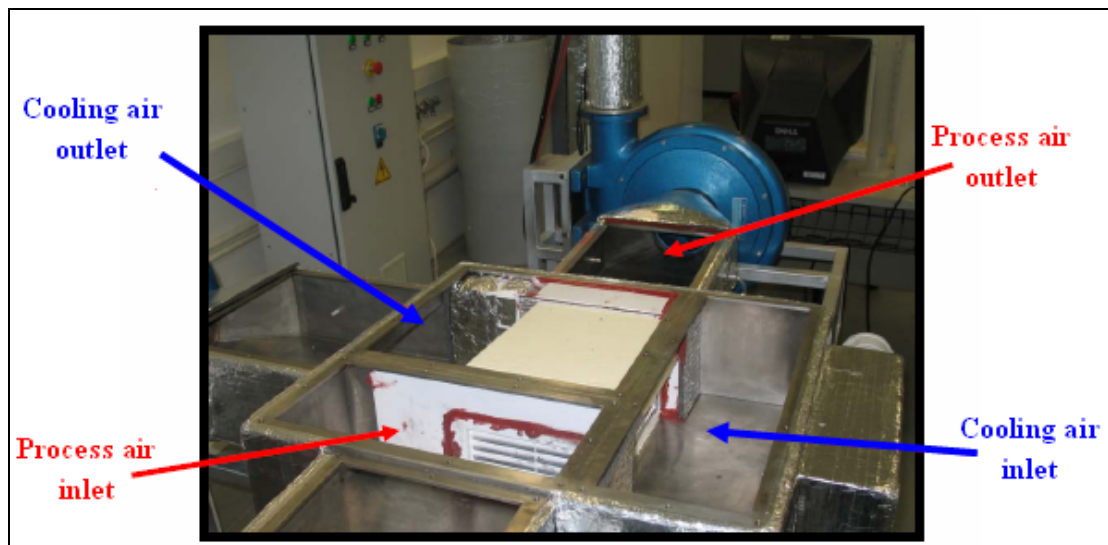


Figure 5.9. The installation of the condenser

#### 5.4.1. Condensation Rate Test Results

With the new prototype condenser, the tests were conducted done with 20 different conditions and each condition was repeated for once. The results for condensation rates are shown in Table 5.4. The mean condensation rate of the 40 test runs was determined to be 0.61 gr/s

Table 5.4. Condensation rate results of the new condenser

Channelp	Channelc	Qp lt/s	Qc lt/s	Tp °C	RHp %	Condensation Rate gr/s	
						Test 1	Test 2
Curved	Curved	30	30	65	95	0,34	0,36
Curved	Curved	30	70	65	85	0,61	0,63
Curved	Curved	42,5	50	70	90	0,60	0,59
Curved	Curved	55	30	75	85	0,43	0,42
Curved	Curved	55	70	75	95	0,99	0,96
Curved	Straight	30	30	75	85	0,41	0,47
Curved	Straight	30	70	75	95	0,93	0,94
Curved	Straight	42,5	50	70	90	0,63	0,62
Curved	Straight	55	30	65	95	0,36	0,35
Curved	Straight	55	70	65	85	0,68	0,64
Straight	Curved	30	30	75	95	0,49	0,45
Straight	Curved	30	70	75	85	0,87	0,85
Straight	Curved	42,5	50	70	90	0,61	0,61
Straight	Curved	55	30	65	85	0,29	0,31
Straight	Curved	55	70	65	95	0,73	0,79
Straight	Straight	30	30	65	85	0,32	0,31
Straight	Straight	30	70	65	95	0,73	0,73
Straight	Straight	42,5	50	70	90	0,61	0,60
Straight	Straight	55	30	75	95	0,51	0,47
Straight	Straight	55	70	75	85	0,91	0,91

After the completion of the tests, results were entered to the Minitab program and a GLM analysis was conducted. As it can be seen from Figure 5.10, all the quantitative factors appear to be effective on the condensation rate. For the new condenser, the channel geometries were found ineffective for the condensation rate while they were effective for the case of the existing condenser. The factors listed in the “Source” column are responsible for 99.24 per cent of the total variation on the condensation rate.

General Linear Model: Cond.Rate versus Qp; Qc; Tp; RHp						
Factor	Type	Levels	Values			
Qp	fixed	2	30; 55			
Qc	fixed	2	30; 70			
Tp	fixed	2	65; 75			
RHp	fixed	2	85; 95			
Analysis of Variance for Cond.Rate, using Adjusted SS for Tests						
Source	DF	SeqSS	AdjSS	AdjMS	F	P
Qp	1	0,00277	0,00277	0,00277	6,62	0,017
Qc	1	1,37079	1,37079	1,37079	3281,12	0,000
Tp	1	0,25362	0,25362	0,25362	607,06	0,000
RHp	1	0,03739	0,03739	0,03739	89,49	0,000
Qp*Qc	1	0,00362	0,00362	0,00362	8,66	0,007
Qc*Tp	1	0,02053	0,02053	0,02053	49,15	0,000
Qc*RHp	1	0,00380	0,00380	0,00380	9,11	0,006
Error	24	0,01003	0,01003	0,00042		
Total	31	1,70255				
S = 0,0204397    R-Sq = 99,41%    R-Sq(adj) = 99,24%						

Figure 5.10. GLM results of the new condenser

For the tests with the new prototype condenser, the condensation rate varies within the range of 0.4-0.8 gr/s. When the effects of the main factors on the condensation rate are closely examined, as shown in Figure 5.11, the cooling air flow rate is determined to be the most effective factor on the condensation rate. The effect of the process air flow rate on condensation rate seems to be negligible.



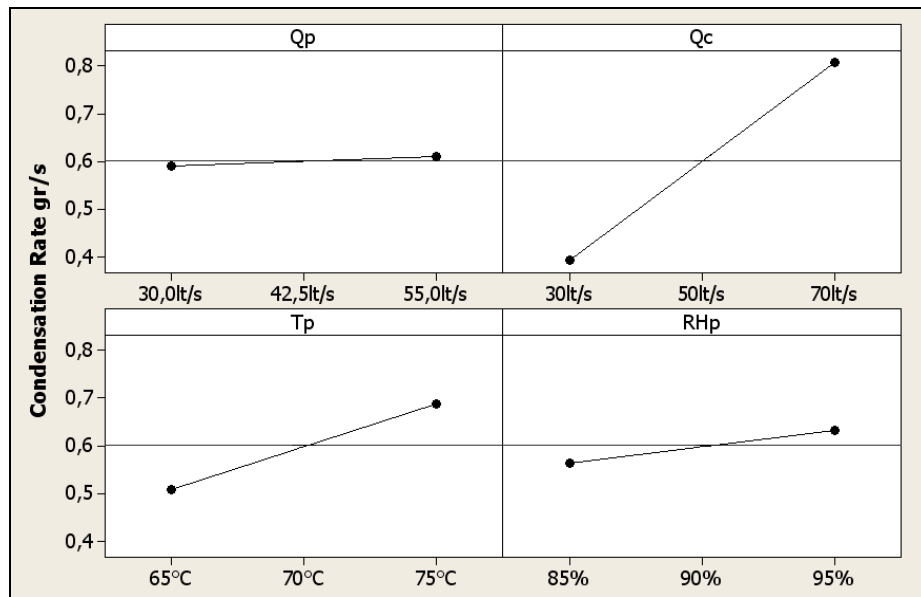


Figure 5.11. Effect of factors on condensation rate

When the effect ratio of each factor is examined, the largest effect ratio on condensation rate is found to be from the cooling air flow rate and the process air temperature. Furthermore, the effect ratio of the other effects and their interactions seems to be insignificant.

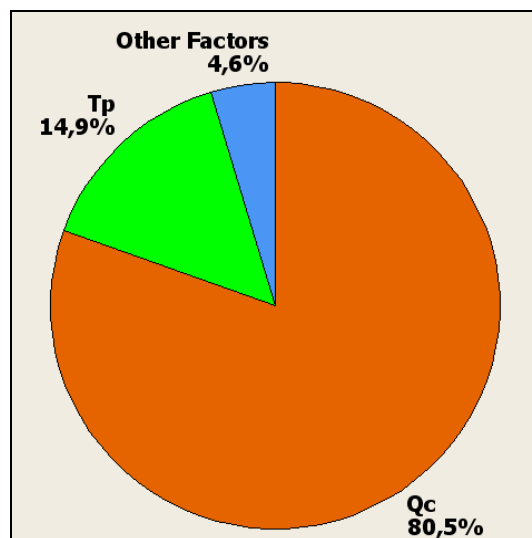


Figure 5.12. Effect ratio of factors on condensation rate

#### 5.4.2. Condenser Efficiency Test Results

After examining the condensation rate of the new prototype condenser with four process and five cooling passes, the condenser efficiency was studied. The efficiency of the condenser was calculated by equations mentioned on Chapter 4.1. The values of the condenser efficiency for the 40 test runs are listed in Table 5.2.

Table 5.5. Condenser efficiency results of the new condenser

Channelp	Channelc	Qp lt/s	Qc lt/s	Tp °C	RHp %	Condenser Efficiency $\eta$	
						Test 1	Test 2
Curved	Curved	30	30	65	95	0,78	0,78
Curved	Curved	30	70	65	85	0,74	0,78
Curved	Curved	42,5	50	70	90	0,75	0,74
Curved	Curved	55	30	75	85	0,80	0,78
Curved	Curved	55	70	75	95	0,79	0,77
Curved	Straight	30	30	75	85	0,77	0,88
Curved	Straight	30	70	75	95	0,79	0,80
Curved	Straight	42,5	50	70	90	0,77	0,79
Curved	Straight	55	30	65	95	0,77	0,74
Curved	Straight	55	70	65	85	0,77	0,71
Straight	Curved	30	30	75	95	0,85	0,80
Straight	Curved	30	70	75	85	0,77	0,76
Straight	Curved	42,5	50	70	90	0,74	0,76
Straight	Curved	55	30	65	85	0,65	0,70
Straight	Curved	55	70	65	95	0,75	0,76
Straight	Straight	30	30	65	85	0,78	0,75
Straight	Straight	30	70	65	95	0,86	0,82
Straight	Straight	42,5	50	70	90	0,76	0,75
Straight	Straight	55	30	75	95	0,85	0,86
Straight	Straight	55	70	75	85	0,77	0,77

The results obtained from the condenser testing unit were then entered to the Minitab program and a GLM analysis was performed. As seen under the “Source” column in Figure 5.13, all the main factors except for the process air condenser inlet channel geometry were found effective on condenser efficiency. The result of the GLM analysis shows that the formed DOE could model the variation of the condenser efficiency with 70.81 per cent.

General Linear Model: Ecooling versus Channelc; Qp; Qc; Tp; RHp						
Factor	Type	Levels	Values			
Channelc	fixed	2	Curved; Straight			
Qp	fixed	2	30; 55			
Qc	fixed	2	30; 70			
Tp	fixed	2	65; 75			
RHp	fixed	2	85; 95			
Analysis of Variance for Ecooling, using Adjusted SS for Tests						
Source	DF	SeqSS	AdjSS	AdjMS	F	P
Channelc	1	0,0059611	0,0059611	0,0059611	8,87	0,007
Qp	1	0,0074567	0,0074567	0,0074567	11,09	0,003
Qc	1	0,0005746	0,0005746	0,0005746	0,85	0,364
Tp	1	0,0136567	0,0136567	0,0136567	20,31	0,000
RHp	1	0,0107518	0,0107518	0,0107518	15,99	0,001
Qp*Tp	1	0,0046958	0,0046958	0,0046958	6,98	0,014
Qc*Tp	1	0,0121712	0,0121712	0,0121712	18,10	0,000
Error	24	0,0161354	0,0161354	0,0006723		
Total	31	0,0714033				
S = 0,0259289    R-Sq = 77,40%    R-Sq(adj) = 70,81%						

Figure 5.13. GLM analysis of the efficiency for the new condenser

The effect of the quantitative factors on the condenser efficiency was examined, and the effect of all the factors seemed to be significant. As it can be seen from Figure 5.14, the condenser efficiency varies within the range of 76 – 80 per cent for all the performed tests. The mean condenser efficiency for these tests was calculated to be 77.5 per cent.

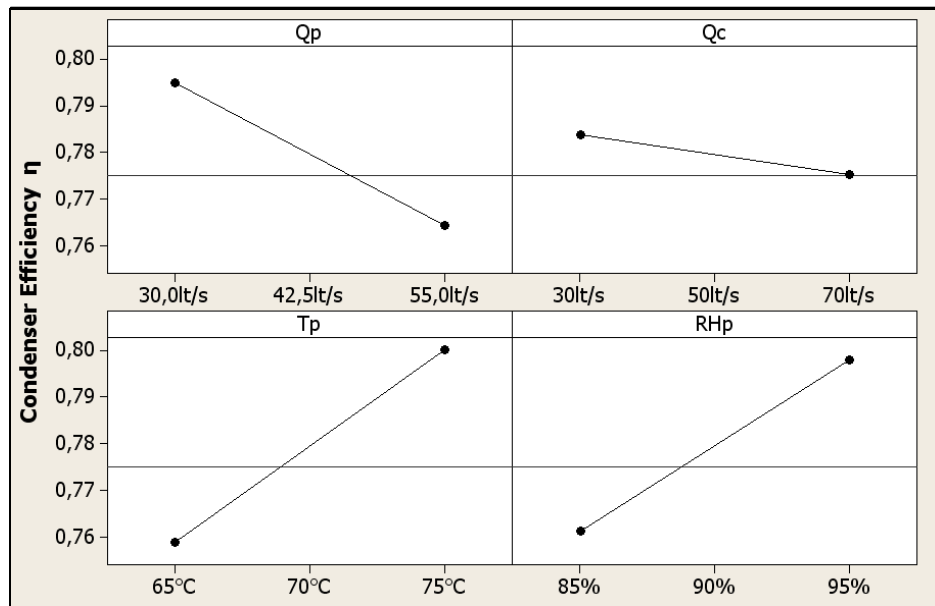


Figure 5.14. Effect of quantitative factors on condenser efficiency

The examination of the effect of the cooling air channel condenser inlet geometry reveals that the cooling air flowing into the condenser with a straight channel yields a higher condenser efficiency than with a curved channel.

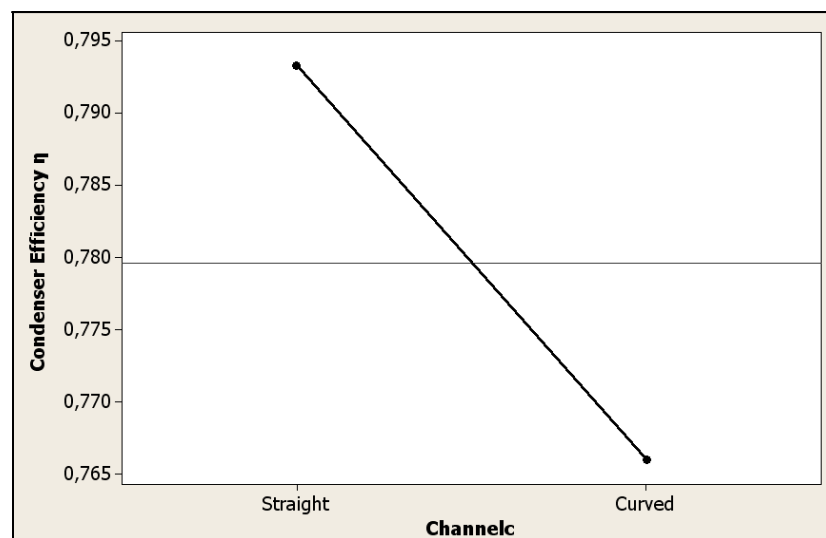


Figure 5.15. Effect of cooling air channel geometry on condenser efficiency.

Figure 5.16 shows the effect ratio of each factor. It seems from the figure that the most effective factor for the condenser efficiency of the new designed condenser is the temperature of the process air at the condenser inlet. Compared to the previous results with the existing condenser, the interaction of the process air temperature with cooling and process air flow rates are also found to be important factors in determining the efficiency of the new condenser.

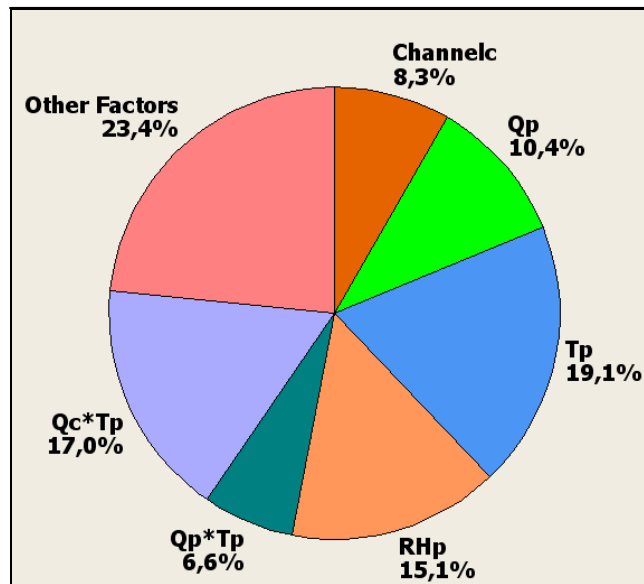


Figure 5.16. Effect ratio of factors and their interactions on condenser efficiency

## 6. EXPERIMENTS ON A TUMBLE DRYER

After getting higher condensation rate and condenser efficiency results with four process pass condenser, it was decided to design a condenser with three process and four cooling passes. As a result of the production constraints, the condenser could not be produced with the intended channel dimensions. As it can be seen from Figure 6.1. the cooling passes of the three process pass condenser was produced by joining two separate fin sets together.

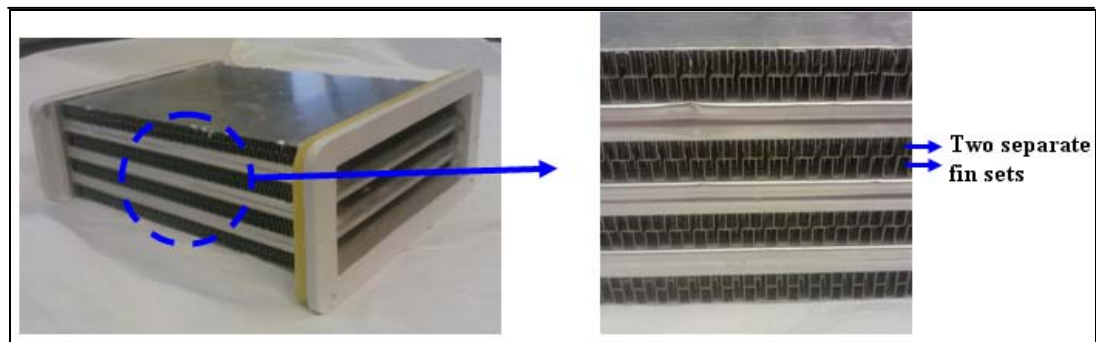


Figure 6.1. Three process pass condenser

The width and the length of the cooling passes were kept the same with the five and four process pass condensers as 235 and 184 mm. The width and the length of the the process passes were chosen as 181 and 277 mm. The height of the process and cooling passes were determined as 12.5 and 11.7 mm.

In the last step of the study five, four and three process pass condensers were tested in a C energy class Beko D 70 Ek air condenser tumble dryer. Five tests were run for each condenser and as it can be seen from Figure 6.2, the highest water collecting efficiency was obtained with four process pass condenser.

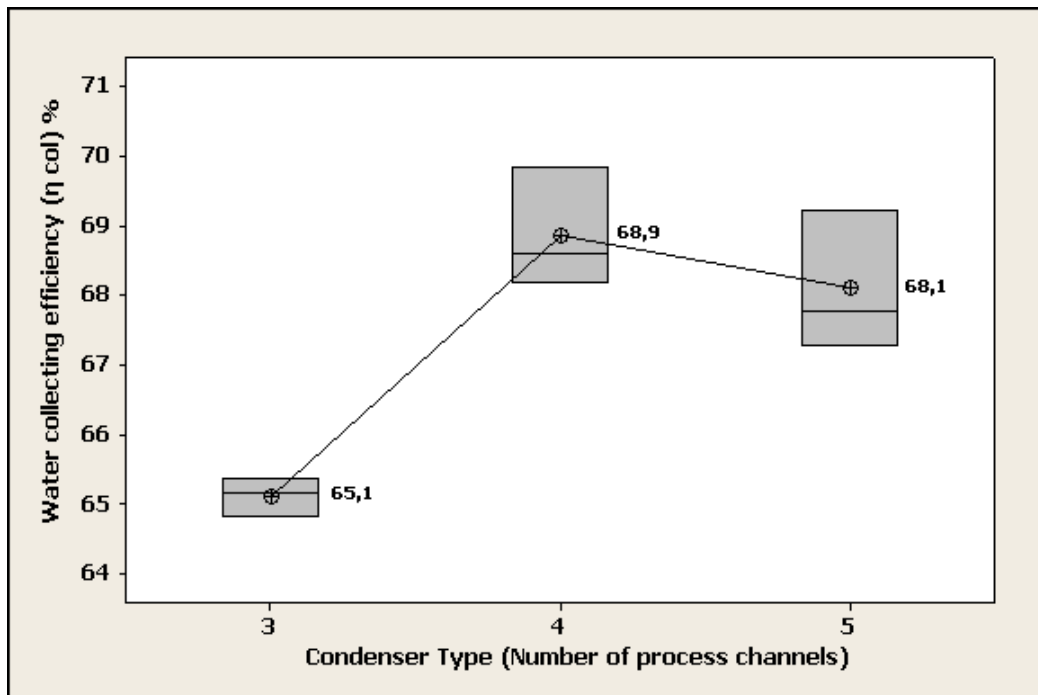


Figure 6.2. Water collecting efficiency test results

As mentioned in Chapter 2 it was known that an increase in the water collecting efficiency effects the energy consumption in a negative way. Despite the increase in the water collecting efficiency of the four and three pass condensers, energy consumption of the machine did not change. When the water collecting efficiency and the specific energy consumption values of the condensers that can be seen on Figure 6.3. were commented together, four pass condenser was the most efficient condenser among the tested ones.

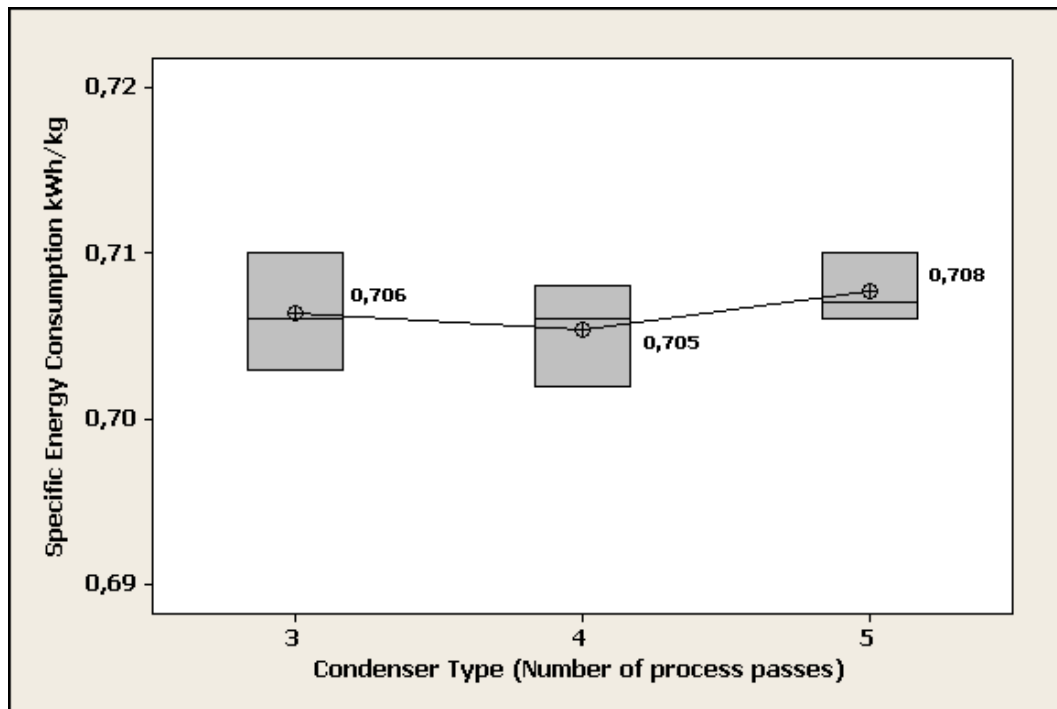


Figure 6.3. Specific energy consumption test results



## 7. CONCLUSION AND FUTURE WORK

### 7.1. CONCLUSION

Rectangular plate fin air-to-air heat exchangers (condensers) were investigated in this project. A simplified air condenser dryer energy model was developed to simulate the effect of the condenser on the energy consumption of an air condenser tumble dryer.

In order to measure the performance of cross flow condensers used in tumble dryers, a condenser testing unit was designed and constructed. A design of experiment (DOE) was formulated and a benchmark condenser with five-process and six-cooling passes was tested under different channel geometries, air flow rates, temperatures and relative humidity values. Total 40 tests were conducted on 20 different conditions, and the condensation rate and the condenser efficiency of the existing benchmark condenser were examined.

Subsequently a new condenser with four-process and five-cooling passes was designed. Due to the dimensional constraints in the dryer, the outer dimensions of the new condenser were kept the same with the existing five-process pass condenser. A simple analysis was conducted to measure the efficiency of a rectangular film, and this analysis was employed to design the fin geometry of the new condenser.

The prototype of the new four-process pass condenser was installed to the condenser testing unit and tested under the same DOE conditions. While the average condensation rate of the existing condenser was measured as 0.58 gr/s, the new designed condenser yielded the condensation rate of 0.61 gr/s. The mean condenser efficiency of the new four-process pass condenser was measured as 77.5 per cent. For the existing five-process pass condenser, this value was 72.7 per cent.

The test results of the five and four process pass condensers indicated that both the cooling air volumetric flow rate and process air temperatures should be increased in order to increase the condensation rate. On the other hand, in order for a higher condenser

efficiency to be achieved, the process air flow rate should be decreased while both the process air temperature and relative humidity should be increased.

In the final step of the study, the existing five-process pass condenser, new designed four-process pass condenser and a three-process pass condenser that was designed by the heat exchanger manufacturer were tested in an air condenser tumble dryer. The minimum energy consumption and the maximum water collecting efficiency rates were achieved with the newly designed four-process pass condenser.

## **7.2. FUTURE WORK**

Designing a condenser for air condenser tumble dryers with higher efficiency and condensation rate was the main motivation of this study. As a future work, it may be necessary to devise an experimental method in order to understand the condensation process within a condenser process channel. Examining the condensation process for different channel lengths, different channel surfaces and different channel heights will provide valuable information on how to increase the condenser performance. For the cooling passes of the condenser, different fin geometries with different fin thicknesses should be examined to optimize the heat removal from process channels. In addition, it may be beneficial to design a dryer simulator which is able to accommodate various condensers with different sizes. This will eliminate a dimensional restriction due to a dryer chassis in the process of designing a better condenser.

## APPENDIX A: COMPONENT SPECIFICATIONS

Table A.1. Isolation material

Material	PE Foam Sheet
Thickness	10 mm
Density	30 kg/m <sup>3</sup>
Conduction Coefficient (TS 388)	0.035 W/(mK)

Table A.2. Temperature and humidity probes

	Process Air	Cooling Air
<b>Company</b>	Rotronic	
<b>Type</b>	Hygroclip M23	Roline 12
<b>Range</b>	0 – 100 RH	0 – 100 RH
	-40 – 85 °C	-40 – 85 °C
<b>Accuracy</b>	± %1 RH	± %0,6 RH
	±0,3 K	± 0,5 K

Table A.3. Differential pressure sensors

	Flow Rate Measurement	Pressure Measurement
<b>Company</b>	ASHCROFT	
<b>Type</b>	Model CXLdp Low Differential Pressure Transmitter	
<b>Range (Pa)</b>	100	250
<b>Accuracy (%)</b>	0,8	0,4
<b>Code</b>	CX8MB242100PA	CX4MB2422500PA

## REFERENCES

1. Ecodesign of Laundry Dryers, “*Preparatory Studies for Ecodesign Requirements of Energy – using – Products (EuP) – Lot 16*”, Task 2 Final Version, June 2008.
2. Hekmat, D., Fisk, W.J., “*Improving the Energy Efficiency of Residential Clothes Dryers*”, NTIS report number LBL 16813, The United States Department of Commerce, Springfield, Virginia, 1983.
3. Conde, M.R., “*Energy Conservation with Tumbler Drying in Laundries*”, Applied Thermal Engineering Vol. 17. No. 12, pp. 1163-1172, 1997.
4. Kao, J.Y., “*Energy Test Results of a Conventional Clothes Dryer and a Condenser Clothes Dryer*”, International Appliance National Conference, 49th Proceedings, pp. 11-21, May 1998.
5. Bansal, P.K., Braun, J.E., Groll, E.A., “*Improving the Energy Efficiency of Conventional Tumbler Clothes Drying Systems*”, International Journal of Energy Research, pp 1315-1332; 2001.
6. Bassily, A.M.; Colver, G.M., “*Correlation of the Area-Mass Transfer Coefficient Inside the Drum of a Clothes Dryer*”, Drying Technology, An International Journal, Vol. 21, No. 5, pp. 919–944; 2003.
7. Bassily, A.M., Colver, G.M., “*Numerical Optimization of the Annual Cost of a Clothes Dryer*”, Drying Technology, An International Journal, Drying Technology, Vol 23, pp. 1515–1540; 2005.
8. Berghel, J., Brunzell, L., Bengtsson, P., “*Performance Analysis of a Tumble Dryer*”, Proceedings of the 14th International Drying Symposium, Vol. B, pp. 821-827, August 2004.

9. Brunzell, L., “*Energy Efficient Textile Drying*”, Karlstad University Studies 2006:61, 2006.
10. Cochran, M.P., “*A Feasibility Study of Incorporating Surface Tension Elements to Improve the Efficiency of Residential Clothes Dryers*”, Kansas State University Thesis Study, 2005.
11. Siow, E.C., “*Numerical Solution of a Two-Phase Model for Laminar Film Condensation of Vapour-Gas Mixtures in Channels*”, The University of Manitoba; 2001.
12. Ormiston, S.J., Siow, E.C., Soliman, H.M., “*Two-Phase Modelling of Laminar Film Condensation from Vapour-Gas Mixtures in Declining Parallel-Plate Channels*”, International Journal of Thermal Sciences, Vol 46, pp. 458–466; July 2006.

**REFERENCES NOT CITED**

*“Format for Theses”*, The Institute of Graduate Studies in Science and Engineering, Yeditepe University Press, 2004.

Kakaç, S., Liu, H., *“Heat Exchangers Selection, Rating and Thermal Design”*, 2<sup>nd</sup> Edition, CRC Pres, 2002.

Shah, R. S., Sekulic, D. P., *“Fundamentals of Heat Exchanger Design”*, WILEY, 2003.

Incropera, F. P., DeWitt, D. P., *“Fundamentals of Heat and Mass Transfer”*, Fifth Edition, WILEY, 2002.